2005

Assessment of brain tumor angiogenesis using perfusion magnetic resonance imaging and magnetic resonance spectroscopy.

Narasimha Shastry Akella
University of Alabama at Birmingham

ASSESSMENT OF BRAIN TUMOR ANGIOGENESIS USING PERFUSION MAGNETIC RESONANCE IMAGING AND MAGNETIC RESONANCE SPECTROSCOPY

by

NARASIMHA SHASTRY AKELLA

A DISSERTATION

Submitted to the graduate faculty of The University of Alabama at Birmingham,
in partial fulfillment of the requirements for the degree of
Doctor of Philosophy

BIRMINGHAM, ALABAMA

2005

ABSTRACT OF DISSERTATION
GRADUATE SCHOOL, UNIVERSITY OF ALABAMA AT BIRMINGHAM

Degree Ph.D Program Biomedical Engineering

Name of Candidate Narasimha Shastry Akella

Committee Chairs Donald B. Twieg, Louis Burt Nabors

Title Assessment of Brain Tumor Angiogenesis Using Perfusion Magnetic Resonance Imaging and Magnetic Resonance Spectroscopy

Magnetic resonance (MR) imaging and spectroscopy have been used to investigate characteristics of brain cancer in vivo, specifically, those arising from angiogenesis, which is thought to be central to tumor growth and invasion. It was established that radiological assessment of angiogenesis is possible with dynamic susceptibility contrast-enhanced MRI (DSC-MRI) in patients with malignant brain tumors.

Thresholds of quality for the T2*-weighted perfusion MRI studies were determined and the effects of an angiogenesis inhibitor on relative cerebral blood flow (CBF) and cerebral blood volume (CBV) changes in patients were evaluated. Quality tests were performed on perfusion data by defining statistical thresholds of acceptance. Region of interest analyses were performed on tumors, and kinetic parameters were normalized with respect to healthy tissue. Decreases in CBF and CBV measurements were observed in patients with clinical response. It was shown that malignant brain tumors have altered perfusion parameters which may be used in the assessment of neovascularization.

The development and testing of a technique to quantify angiogenesis in brain tumor patients using perfusion MR data is presented and used to examine the spatial variance of angiogenesis. The angiogenesis potential, $\mathcal{A}$, was computed for each pixel. A concentric annular model is proposed to evaluate the spatial variance of $\mathcal{A}$. Inter-patient

data was used to assess the spatio-temporal patterns of hemodynamics in malignant tumors. It is possible to quantify angiogenesis on a pixel-by-pixel basis using hemodynamic measures such as CBF, CBV, and T2* recovery. Malignant brain tumors have remarkable similarity in the spatial distribution of their angio-architecture. Longitudinal changes in angio-architecture can also be monitored using this method.

In the final phase, tumor hemodynamics are correlated with metabolite distributions, acquired using chemical shift imaging. The levels of N-acetyl aspartate (NAA) and choline (Cho) are found to be significantly lower in the tumor core, where CBF is very low. In the tumor fringes, where angiogenic activity is presumably high, increased CBF corresponded to increased Cho and decreased NAA. The angiogenesis potential was also compared with Cho/NAA ratio images. Hemodynamic and spectral data concur in brain tumors with respect to their spatial variation.

DEDICATION

This doctoral dissertation is dedicated to *Amma* and *Nanna,* for their inspiration, teaching, and encouragement; brain cancer patients and their families; and, researchers worldwide, whose tenacious efforts to combat brain cancer have provided hope and cheer to those ailing from this deadly disease.

ACKNOWLEDGMENTS

I would like to express sincere gratitude to my research advisors, Dr. Donald B. Twieg and Dr. L. Burt Nabors. They have both been superb teachers and excellent mentors. I also thank the other members of my doctoral committee, Dr. Edward G. Walsh, Dr. Joel K. Curé, and Dr. Bradley R. Newcomer for several useful discussions which have strengthened this dissertation significantly.

I thank the faculty, staff, and students of the Department of Biomedical Engineering at UAB for their support and camaraderie. I have made some great friends during my stint in the department, and carry forward several fond memories from my days in graduate school. Special thanks are due to Thyrza Johnson, Shirley Gibbs, and Jolene Lewis for their help with administrative, financial, and regulatory paperwork.

I consider myself very fortunate to be surrounded by people who understand and appreciate the rigors of doctoral studies, especially my parents, who have been unwavering in their support of my academic pursuits. They were my first teachers and continue to inspire me to be the best I can be. I also thank my brother for his support and encouragement. I would also like to thank my best friend Manasi for her help with compiling this work and for putting up with me in a way only she can. I could not have finished this endeavor without these people, and I remain forever indebted to them for everything they have done.

Individuals who assisted with various phases of this work are acknowledged in the reprints/preprints presented in this dissertation.

TABLE OF CONTENTS

Page

LIST OF TABLES

LIST OF FIGURES

LIST OF FIGURES (Continued)

LIST OF ABBREVIATIONS

AA	Anaplastic Astrocytoma
ADC	Apparent Diffusion Coefficient
AIF	Arterial Input Function
CBF	Cerebral Blood Volume
CBV	Cerebral Blood Flow
CHESS	Chemical Shift Selective Saturation
CSI	Chemical Shift Imaging
DICOM	Digital Imaging and Communication in Medicine
DSC-MRI	Dynamic Susceptibility Contrast enhanced MRI
EPI	Echo Planar Imaging
FA	Fractional Anisotropy
FLAIR	Fluid Attenuated Inversion Recovery
FOV	Field of View
GE	Gradient Echo
GBM	Glioblastoma Multiforme
ICA	Independent Component Analysis
MION	Monocrystalline Iron Oxide Nanocompounds
MRI	Magnetic Resonance Imaging
MRS	Magnetic Resonance Spectroscopy
MRSI	Magnetic Resonance Spectroscopic Imaging

MTT	Mean Transit Time
NAA	N-acetyl aspartate
PCA	Principal Component Analysis
ROI	Region of Interest
SE	Spin Echo
SNR	Signal to Noise Ratio
T1WI	T1 weighted image
T2WI	T2 weighted image
TE	Echo Time
TR	Repetition time
UAB	University of Alabama at Birmingham
VOI	Volume of Interest
WHO	World Health Organization

INTRODUCTION

Brain tumors have been extensively investigated using magnetic resonance-based techniques because they afford excellent tissue contrast, spatial resolution, and sensitivity. Advances in hardware and software have led to faster and more efficient magnetic resonance imaging (MRI) and magnetic resonance spectroscopy (MRS). This, in turn, has led to new approaches that enable us to evaluate the functionality, patho-physiology, biochemistry, and metabolism of tumors in vivo.

Ever since it was postulated in the early 1970s that tumor-associated angiogenesis is critical to growth and invasion of cancer (1), researchers have investigated aspects of brain tumors that shed light on the metabolism associated with brain tumor angiogenesis. The chief aims of this work were to design, implement, and test MRI/MRS techniques to quantitatively assess angiogenesis in vivo. The broad goals were as follows:

1. Establishing the role of quantitative cerebral hemodynamics as surrogate markers of brain tumor angiogenesis using perfusion MRI,
2. Developing postprocessing techniques to interrogate this data for spatio-temporal information and attempt to quantitate angiogenesis on a pixel-by-pixel basis, and,
3. Correlating hemodynamic data with MRS/Spectroscopic imaging data in an attempt to understand the spatial variation of angiogenesis-related biochemistry and its relation to hemodynamic variations in brain tumor patients.

Accomplishing the aforementioned goals has been facilitated by development of new techniques, modifications of existing algorithms, and image postprocessing ap-

proaches, statistical validation and testing, and correlations of imaging and clinical data. Each of these tasks is presented in the reprint/preprint format. The computer programming for data analyses was done in MATLAB (The MathWorks Inc., Natick, MA). Other commercial packages have been used and are reported in the reprint/preprints.

Brain Tumors

Primary brain cancer affects over 40,000 people in the United States each year. Of those, it is estimated that around 18,000 cases will be malignant glioma. These include anaplastic (malignant) astrocytomas (AA), oligodendrogliomas, and glioblastoma multiforme (GBM), the three types of tumors that account for a majority of the patients studied in this work. Table 1 shows the most common types of brain tumors, their characteristics and imaging features. Brain tumors are the second most common cancer of children, the third most common cause of death for adults ages 15-34, and the third leading cause of years-of-life loss related to cancer. This is a tremendous toll given the relatively low incidence. Survival for patients remains poor, with little improvement over the past twenty years despite advances in therapeutic strategies, surgery, radiation, and chemotherapy. Significant improvements in treatment options and patient outcomes will require advances in our understanding of the functionality of tumors and their pathophysiology and biochemistry. Conceivably, this will not be possible without advances in imaging and spectroscopy methodologies.

The hallmarks of malignant brain tumors are invasion and endothelial proliferation (2). The clinical features of a large, enhancing mass with destruction of normal brain are a common presentation for patients with primary brain cancer. Malignant gliomas are

Table 1 Feature Summary of Brain Tumors.

Tumor Type	Clinical Characteristics	Imaging Features
Pilocytic Astrocytoma	• Well circumscribed tumors • Less biologically aggressive • Favorable prognosis • Typically located in the midline, optic pathways, thalamus and brain stem • Occur in children and young adults	• Tumor nodules show intense enhancement • Cysts are hypointense on T1-weighted images (T1WIs) and hyperintense on T2-weighted images (T2WIs) • Not radiographically cystic
Astrocytoma (WHO grade II)	• Diffusely infiltrating tumors composed of neoplastic astrocytes • Occur in early to mid adult life • Microscopically ill-defined • 3 major histopathological variants: fibrillary, gemistocytic, and protoplasmic • Usually superficial in location and may involve overlying gray matter	• Calcification present in 50% of the case, though seldom appreciated in MRI • Well-defined homogenous masses • Hypointense on T1WI and hyperintense on T2WI • Enhancement is variable
Anaplastic Astrocytoma (WHO grade III)	• Occur later in life than grade II tumors • Pathologically, they have increased hypercellularity, pleomorphism, and mitosis • Necrosis and endothelial proliferation are absent	• Heterogeneous on MRIs • Less well-defined borders and greater mass effect, vasogenic edema and enhancement • In non-contrast T1 and T2 images heterogeneous signal intensity is present
Glioblastoma Multiforme (WHO grade IV)	• Most common astrocytic tumor • Peak incidence is at age 45-60 • Occurs in the frontal lobe, cerebellum, brain stem and spinal cord. • Spreads across white matter tracts to involve contralateral hemisphere (butterfly appearance) • Pathologically heterogeneous with areas of necrosis, hemorrhage, and endothelial proliferation • Spreads to subarachnoid space	• MRI reflects heterogeneous pathology – heterogeneous signal intensity on both T1WIs and T2WIs • Poorly defined with mass effect and vasogenic edema • Hemorrhage is common and useful in distinguishing from lower grade astrocytomas • Signature: large region of high signal on T2WIs (edema + microscopic tumor infiltration) • T2 FLAIR provides good visualization
Oligodendrogliomas	• Uncommon (4% to 7% of intracranial gliomas) and slow growing • Symptoms include long history of seizures and (rarely) headaches • Occur mostly in the peripheral aspects of the frontal and parietal lobes • Solid, infiltrative lesions with well-defined borders • Generally round or oval	• High degree of calcification • Heterogeneous in signal intensity • Predominantly isointense with gray matter on T1WIs and hyperintense on T2WIs • GE imaging is more sensitive to calcification and hemorrhaging than SE and is useful in visualizing these tumors • 50% demonstrate faint enhancement

intensely angiogenic cancers. Clinical morbidity and mortality are related to the degree of angiogenesis for astrocytomas. Most patients who were evaluated as a part of this study had diagnoses of malignant tumors such as AA and GBM, World Health Organization (WHO) grades III and IV, respectively. Patients typically have very low 1-year survival rates and usually receive a multitude of therapeutic interventions: chemo-therapy, radiation, anti-angiogenic drugs, and/or surgery.

The non-invasive measurement of the extent of a brain tumor and its radiological characteristics at diagnosis and during the clinical course is critical to the understanding of clinical remission and, therefore, to the therapeutic response or failure and malignant progression.

Angiogenesis

Angiogenesis is an essential component of tumor progression in which neovasculature nourishes growing tumors and facilitates tumor expansion beyond 2 mm^3 (3-5). Malignant tumors are among the best vascularized tumors in humans (6). Several researchers have focused on studying mechanisms of tumor vascularization, including studies of the growth factors and receptors involved. These efforts have resulted in various approaches for anti-angiogenic treatment of brain tumors (7) and new approaches for such therapy are constantly evolving. Cytotoxic chemotherapy has limited activity against malignant gliomas. The blood brain barrier is partially responsible for the difficulties with delivery of drugs to brain tumors and, thus, for some of the ineffectiveness of such therapy.

Angiogenesis-inhibiting agents like EMD121974 (cilengitide, a synthetic pentapeptide, manufactured by Merck KgaA, Darmstadt, Germany), administered to brain tumor patients in the preliminary stages of this research, are particularly promising for primary malignant brain tumors. This is because malignant brain tumors have significant neovascularization and the blood brain barrier does not have to be crossed to reach the target cells.

Malignant glial tumors are characterized by their angiogenic behavior, and the modulation of angiogenesis may be particularly effective in their treatment (8). The complex angio-architectural arrangements accompanying brain tumor growth usually have three components: tumor associated angiogenesis, tumor-induced vascular modifications, and vascular expansion.

The key to evaluate angiogenesis in vivo is identifying parameters that quantify the hemodynamics of brain tumors reliably. We have used blood flow and volume extensively throughout this work, in addition to a couple of other indices. Additional measures of microvascular permeability, diffusion, and histological markers could be used to complement hemodynamic observations. It must be pointed out, however, that most imaging techniques used to study tumor vascularization fail to delineate the heterogeneity inherent to tumors and, hence, do not fully reveal their spatial characteristics.

MRI and MRS

Several MRI and MRS techniques have been successfully devised to study brain tumors in a clinical setting, ranging from radiological diagnosis to tumor characterization and from size and volume computations to measurement of bio-chemical information. In

this work, we investigate angiogenesis in primary malignant brain tumors using a combination of perfusion MRI and MRS. The non-invasive nature of an MRI examination allows for longitudinal acquisition of data, which in turn allows for monitoring of disease progression and/or therapy tracking. The preliminary MRI studies reported in this dissertation were performed at a field strength of 1.5T. Spectroscopic imaging and the correlating perfusion dynamic susceptibility contrast-enhanced MRI (DSC-MRI) studies were performed at 3.0T.

Perfusion is the steady-state delivery of blood to tissue parenchyma through the capillaries, representing the microscopic coherent motion of water and cellular material (9). We use perfusion imaging to correlate angiogenesis and kinetic parameters reflecting tumor vasculature changes. The validation of functional MRI techniques like DSC-MRI for assessment of anti-angiogenic response in brain tumors, and the development of sophisticated postprocessing algorithms to extract and interpret functional and biochemical information, will be required to move novel brain tumor therapy to comparative trial testing.

Early applications of dynamic T2*-weighted perfusion MR imaging have shown that bolus administration of a paramagnetic contrast medium can be used to quantify regional blood flow and volume (10,11). The variations in signal intensity of the brain tissue and blood vessels during the first pass of the contrast agent are due to local field inhomogeneity. Under such circumstances, it has been demonstrated that the acquired T2*-weighted images provide information about blood flow dynamics *in vivo*.

As evidence mounts that techniques like DSC-MRI can be used to aid clinical diagnosis and interpretation of human brain tumors, more focus is being placed on understanding the basic molecular pathways and cellular processes involved. Towards this end,

understanding angiogenesis, i.e., the process of vascularization of tissue involving the development of new capillary blood-vessels, is very important.

In tumor-induced angiogenesis, especially in malignant brain cancer, the capillaries have discontinuous basement membranes that lack a blood-brain barrier. These abnormal capillaries permit diffusion of contrast agents such as Gd-DTPA into the extravascular space, which leads to the classic contrast enhancement on MR images. The areas of the greatest enhancement usually correspond to areas of the tumor that have the greatest blood-brain barrier disruption.

MRS or MR spectroscopic imaging is, like conventional MRI, a non-invasive method to map the distribution and measure concentrations of cerebral metabolites. Several nuclei have been tapped for spectral acquisitions but ^{1}H (proton) spectroscopy techniques are best suited for brain pathologies, given the abundance of hydrogen in brain tissue. The utility of using spectroscopy in studies of brain tumors has been well-documented (12). Spectroscopy is currently being investigated as a tool to research brain tumor heterogeneity and the biochemical changes associated with tumor pathology. Metabolites like choline, N-acetyl aspartate (NAA), creatine, and lactate, which have been implicated in brain tumor metabolism, are routinely imaged using techniques like chemical shift imaging (CSI), which enable multi-voxel acquisitions of fairly robust spectra (13). These spectra can then be used to generate metabolite images and/or, with the help of sophisticated time-domain analyses, be processed to quantitate metabolite concentrations in vivo.

An understanding of the dynamics of angiogenesis cannot be achieved without an integrated analysis of morphological, functional, and molecular approaches that shed light on changes in tissues. Functional characterization of the tumor neovasculature by

imaging will be important for the evaluation of patients receiving anti-angiogenic therapy. Interest in imaging techniques that can provide early indicators of effectiveness at a functional or molecular level has therefore increased. Tumor response to treatment can be detected by functional imaging techniques that are capable of monitoring changes such as perfusion, blood volume, or micro-vessel permeability. MRI can measure both blood volume and blood vessel permeability using dynamic enhancement with extra-cellular or blood pool contrast agents. Contrast-enhanced MRI can distinguish between normal and malignant tissues reflecting the hyper-permeable tumor vasculature. Contrast uptake correlates with micro-vessel density in human and animal experimental tumors. This is the basis for attempting to understand and track angiogenesis using non-invasive imaging techniques like perfusion imaging.

Potential applications for such work would include tumor diagnoses, grading, surgical planning, and radiation therapy, as well as the ability to quantify the functional efficacy of cancer drugs targeted at specific molecular and cellular processes like angiogenesis inhibitors.

Human Subject Data Integrity

Since a large volume of medical imaging data was handled, we used the digital imaging and communication in medicine (DICOM) standard for data storage, retrieval, and processing. All patient data was handled in compliance with the health information portability and accountability act (HIPAA) and utmost care was taken to ensure patient confidentiality. All patient-identifying information such as name and medical record number were stripped from the imaging and spectroscopy data sets and data processing

was performed on University of Alabama at Birmingham (UAB)-owned computers, data-devices, media, and peripherals only.

All the imaging and spectroscopic data acquisition was conducted after obtaining informed consent from the patients. Data handled as a part of this research project were used for secondary analyses only and can not be linked to the human subject from which they were obtained. The protocols used were approved by the UAB Clinical Trials Review Committee, and the UAB Institutional Review Board, overseeing all human experiments. A letter from the Institutional Review Board indicating permission for use of the data for this dissertation, along with copies of the original approval certification used for obtaining data are attached in the appendix.

Overview of Dissertation Research

The chief motivation behind the quantitative investigation of tumor metabolism is a better understanding of the patho-physiology and response to therapy. This will enable better planning and treatment of these tumors. Measures of cerebral hemodynamics such as relative CBF and relative CBV, response to exogenous contrast agents, and spatial variations in quantitative indices of angiogenesis and similar variations in metabolite concentrations are the focus of this study and, in the context of angiogenesis, provide valuable information about tumor metabolism. For MR techniques to be able to measure physiological changes that occur in response to anti-angiogenic/anti-vascular effects, several developments are needed (14), including correlation of measurements, standardized evaluation and modeling techniques, and co-registration of images for comparison. This dissertation is a compilation of techniques developed, implemented, and tested towards these goals.

This dissertation is divided into three main sections. The first goal was to establish proof of principle that DSC-MRI using T2* susceptibility physics could be used to assess angiogenesis in brain tumor patients by utilizing the CBF and CBV as end-points, i.e., a statistical marker of the clinical outcomes in patients. This was accomplished in a multi-institution study of the National Cancer Institute/New Approaches to Brain Tumor Therapy consortium and is reported in the first article, published in the *Journal of Magnetic Resonance Imaging* in 2004 (15). Radiological and clinical observations are in agreement with regards to efficacy of the anti-angiogenic drug cilengitide.

While the CBF and CBV reveal functional information about brain tumors, they do not provide details about the spatio-temporal variation of hemodynamics. To the best of our knowledge, there are no known postprocessing techniques that provide a quantitative insight into angiogenesis using perfusion MRI data. The second goal was to develop a framework whereby such information could be extracted from the DSC-MRI studies on brain tumor patients. Based on response to administration of gadolinium contrast agents, the behavior of parameters like CBV and CBF were utilized to develop a formalism to quantify angiogenesis. These results are reported in the second manuscript of the dissertation. An abstract summarizing our technique (16) has been accepted for presentation at the International Society for Magnetic Resonance in Medicine's 2005 annual meeting and will be submitted to the *Journal of Magnetic Resonance Imaging* as a full-length original research paper.

Another critical aspect of the study of angiogenesis is the assessment of cerebral biochemistry. This is done by mapping metabolites like NAA, choline, creatine, etc. to evaluate their distributions. We acquire such information using CSI and report their correlation with hemodynamic information in the third manuscript of the dissertation. This

attempt to correlate spectral information with the hemodynamic information was taken up as a pilot study in two brain tumor patients. With the feasibility of such acquisition and analyses confirmed, studies involving MRI/MRS are ongoing and patient accrual is currently open. The results will be submitted to *Magnetic Resonance Imaging* for possible publication.

ASSESSMENT OF BRAIN TUMOR ANGIOGENESIS INHIBITORS USING PERFUSION MAGNETIC RESONANCE IMAGING: QUALITY AND ANALYSIS RESULTS OF A PHASE I TRIAL

by

N. SHASTRY AKELLA, DONALD B. TWIEG, TOM MIKKELSEN,
FRED H. HOCHBERG, STUART GROSSMAN,
GRETCHEN A. CLOUD, AND L. BURT NABORS

Journal of Magnetic Resonance Imaging Vol. 20, 913-922

Format adapted and errata corrected for dissertation

ABSTRACT

Purpose: To determine thresholds of quality for a T2*-weighted perfusion magnetic resonance imaging (MRI) study and evaluate the effects of an angiogenesis inhibitor on relative blood flow and volume changes in brain tumor patients, in a multi-institution setting.

Materials and Methods: A total of 36 volunteers from four participating institutions with clinically diagnosed malignant gliomas were studied using perfusion MRI protocols. These included a baseline study and follow-up studies every eight weeks to evaluate the effect of an anti-angiogenic agent on tumor perfusion. Quality tests were performed on the perfusion imaging data by defining statistical thresholds of acceptance. Region of interest (ROI) analysis was performed on tumors and kinetic parameters were normalized with respect to normal tissue.

Results: Statistical thresholds for goodness of the gamma variate fit, T2* recovery, and mean signal full-width half-minimum (FWHMin) were computed for our data sets with a 99% one-sided confidence interval; these were 6.91%, 79.48%, and 23.35 seconds respectively. Decreases in blood volume and flow measurements were observed in patients with documented clinical response.

Conclusions: Malignant brain tumors have altered perfusion parameters that may be used to understand and monitor neovascularization. This permits non-invasive assessment of the efficacy of angiogenesis inhibiting drugs.

INTRODUCTION

Several magnetic resonance imaging (MRI) techniques have been successfully devised to study brain tumors in a clinical setting ranging from radiological diagnosis,

description of tumor characteristics, evaluation of size and volume, and determination of biochemical information. The chief advantage of using MRI over other imaging modalities is the excellent soft tissue contrast it affords coupled with very good resolution and sensitivity. This work describes an attempt to acquire and analyze perfusion MRI data from patients with primary brain tumors that were enrolled in an early phase clinical trial of the anti-angiogenic compound, EMD 121974 (cilengitide). This was done to establish statistical quality metrics and evaluate the effects of cilengitide therapy on relative cerebral blood flow (CBF) and cerebral blood volume (CBV) changes in these patients.

Angiogenesis is an essential component of tumor progression in which neovasculature nourishes growing tumors and facilitates tumor expansion beyond 2 mm^3 (1-3). Malignant gliomas are among the best vascularized tumors in humans (4,5). Angiogenesis inhibiting agents, like EMD 121974 used in this study, are particularly promising for brain tumors because these tumors have marked neovascularization, significant molecular alterations producing an angiogenic and invasive phenotype, and a poor clinical outcome that correlates with an angiogenic phenotype (6,7).

Perfusion is the steady state delivery of blood to tissue parenchyma through the capillaries (8). Perfusion MRI may be used to evaluate kinetic parameters of blood in normal and pathological conditions of the central nervous system. Applications of perfusion MRI like dynamic susceptibility contrast-enhanced MRI (DSC-MRI) have shown that bolus administration and tracking of a paramagnetic contrast medium can be used to quantify regional blood flow and volume (9-13).

Contrast-enhanced MRI has been used to evaluate tumors by several groups primarily to characterize tumor vascularization and flow properties and correlate these with histologic grade (14-17). Daldrup et al (14) have shown a highly positive correlation be-

tween tumor permeability to macromolecular contrast medium and tumor grade. MR-derived relative CBV maps have also correlated with histological measures of microvessel density from surgical tissue in the evaluation of tumor angiogenesis (15). Sugahara et al (18) demonstrated a relationship in astrocytic gliomas between the maximum CBV and histological vascularities that correlated with tumor grade. Others have used T2*-weighted MRI perfusion sequences for generating blood volume maps to improve the accuracy of stereotactic biopsies. Knopp et al (19) used areas of perfusion abnormality to aid targeting of biopsies in patients with astrocytomas. T2*-weighted perfusion methods have also been shown to be effective in computing permeability of high and low grade glial neoplasms while being consistent with earlier results reported using T1-weighted methods (20).

Maximum signal drop and area under the signal-time curve have been monitored to provide information about blood kinetics (21). The blood volume of glioblastoma multiforme (GBM) has been evaluated both qualitatively and quantitatively using dynamic perfusion-weighted imaging and it was shown that double-echo imaging may be more suitable for analysis of blood volume in GBM (22). Other attempts have been made to quantify fractional volumes of different glioma compartments as well as vessel permeability and CBF using T1-weighted dynamic MRI towards pharmacokinetic characterization of gliomas (23). Variations in the recirculation characteristics of a contrast agent bolus have been related to tumor grade in gliomas. Abnormalities in contrast agent recirculation (24) provide independent information concerning the microcirculation in imaging studies of angiogenesis and may be useful in the assessment of trials of anti-angiogenic therapies like the one attempted in this study. DSC-MRI techniques have been tested as surrogate markers of tumor response to anti-angiogenic therapy in xenograft models of

human gliomas (14, 25) and reductions in relative CBV correlated well with tumor response.

Functional perfusion imaging allows for the evaluation of the whole tumor and not selected areas biased by biopsy samples. However, the use of imaging based surrogate markers for the assessment of the angiogenic process is strongly dependent on their test-retest reproducibility. Jackson et al (26) have formally tested the reproducibility of T2* blood volume and vascular tortuosity maps in cerebral gliomas and concluded that measurement of relative blood volume in consecutive studies is statistically capable of reliably detecting changes in excess of 15% in between group studies and 25% in individual patients.

In this report, we evaluated the acquisition and analysis of DSC-MRI in a multi-institutional setting. We will report on the statistical analysis of DSC-MRI data sets from a clinical trial and our attempt to define thresholds for quality and reliability. For those studies that meet the threshold measures, we have analyzed for perfusion parameters in a large population of recurrent malignant gliomas. This represents one of the first efforts to apply the principles of DSC-MRI to the clinical issue of early phase assessment of anti-angiogenic agents.

MATERIALS AND METHODS

EMD 121974 (Cilengitide): Angiogenesis Inhibitor

EMD 121974 is a synthetic pentapeptide supplied in solution form for parenteral administration (Merck KgaA, Darmstadt, Germany). It is supplied by the Division of Cancer Treatment and Diagnosis (DCTD), National Cancer Institute (NCI), as an isotonic solution containing 450 mg of lyophilized EMD 121974 dissolved in 30 mL of sodium

chloride and water for injection (at a concentration of 15 mg/mL). This angiogenesis inhibitor is a potent and selective αvβ3 and αvβ5 vitronectin receptor antagonist.

Patients who were eligible to receive the drug were enrolled in NABTT 9911: A Phase I study of EMD 121974 for patients with recurrent malignant glioma, conducted by the NCI Central Nervous System Consortium, New Approaches to Brain Tumor Therapy (NABTT). The clinical trial used a standard phase I dose escalation design. EMD 121974, with a starting dose of 120 mg/m^2, was administered twice a week, intravenously, over one hour. The dose of the drug was escalated in a stepwise fashion. The first five dose levels were 120, 240, 360, 480, and 600 mg/m^2. The protocol was subsequently amended to allow for further dose escalations leading to dose levels of 1200, 1800, and 2400 mg/m^2.

Perfusion MRI

The perfusion imaging sequences were run on 1.5 T scanners of different manufacturers–GE (Signa 5.7, GE Medical Systems, Milwaukee, WI), Siemens (Magnetom Vision, Siemens Medical Systems, Erlangen, Germany), and Philips (Gyroscan ACS-NT, Philips Medical Systems, Best, The Netherlands)-depending depending on trial site. A total of 36 patients with clinically diagnosed malignant gliomas were imaged during multiple sessions. These included a baseline scan before first administration of the angiogenesis inhibitor and follow-up perfusion scans performed after every eight weeks of treatment with EMD 121974. Twenty-one patients were imaged multiple times, while the others had only a baseline scan.

There were a total of 72 perfusion MRI studies analyzed during the preliminary phase of this work. Due to the multi-institution setting of this study, the DICOM (digital

imaging and communication in medicine) standard was used for image storage, exchange, and query. The chief objectives of the DICOM standard are to achieve compatibility and improve the reliability and efficiency between imaging acquisition systems and other information systems like picture archiving and communication systems in healthcare environments worldwide.

The gradient recalled echo-planar imaging (EPI) sequence was used for acquiring functional perfusion data. This study used a TR of 1900 msec and a TE of 50 msec, accommodating a 20% variation in both TR and TE to permit machine/trial site specific acquisition settings. A 24 cm x 24 cm field of view was used and 5-10 (depending on the size of the tumor) 6- to 8-mm axial slices passing through the center of the tumor were imaged over 40 to 65 functional time points resulting in a total scan time of just over two minutes. In some instances, the tumors were larger than the volume imaged by five slices; in such cases, a greater number of slices were imaged and then the five contiguous slices with the highest mean blood flow and volume were utilized for interpatient analyses of the hemodynamics.

Spin-echo (SE) postcontrast T1-weighted images were acquired following perfusion imaging for anatomic reference. These images were acquired with a TR of 450 ms and TE of 10 ms. The standard dose of the gadolinium based contrast agent was 0.2 mmol/kg of patient body weight. The contrast agent was injected with a power injector at a flow rate of 4.0 mL/sec and an injection delay of 15 seconds.

Perfusion Analysis

Post processing and perfusion analysis was performed using the MedX software (version 3.4.2, Sensor Systems, Sterling, VA) running on a Sun Blade 1000 workstation (Sun Microsystems, Palo Alto, CA) with the Solaris 8 Operating System.

Each of the *N* anatomic slices imaged at 40-65 time points were used to generate a statistical mean image in preparation for temporal plotting of the susceptibility curves. These mean functional images are then inspected for quality, contrast agent induced susceptibility behavior, and artifacts. In agreement with the theoretical models available, five distinct features were observed (8,27):

1. A baseline phase consisting of the signal before contrast agent arrives in the tissue,
2. Arrival of the contrast agent triggering a drop in signal intensity,
3. Maximum signal drop that occurs when the highest concentration of contrast agent is present in the blood vessels,
4. A wash out phase marked by a recovery of the signal, and finally,
5. A postinjection signal that is slightly lower than the preinjection baseline because the concentration of the gadolinium is still sufficient to cause a slight signal drop.

The data sets were prepared for post-processing by inspection for quality, masking, and generation of parametric maps. Masking of the functional data based on an empirically determined threshold was performed to ensure accurate determination of arterial input function and to avoid curve-fitting of pixels outside the brain. A two-stage automatic algorithm (28) was used for identifying arterial voxels in the DSC-MRI data and constructing the arterial input function (AIF). This method uses multiple "arterial likelihood" metrics to choose the best candidate input function for computing the AIF. Motion

correction and spatial filtering were not performed. The arterial and mean tissue curves are computed based on the signal-time curves. The arterial likelihood map was computed based on maximizing P(large peak-height), where P represents the probability. Of the top 45 pixels in the selected arterial likelihood map, the first 20 pixels were excluded as noise and the next 25 were averaged to create the input function. The relative CBV maps are determined though gamma variate fitting (29) of the concentration curves and integration. The relative CBF maps are generated from the amplitude of the residue curve which results from deconvolution of the tissue curve via singular value decomposition. A three-point temporal smoothing is applied prior to analysis and a constant noise model is assumed. Fitted measures and goodness of fit were computed for each data set.

A three parameter gamma variate model (Eq. [1]) was used for computing the contrast agent concentration curve $C(t)$:

$$C(t) = K\,\tau^{\beta}\,e^{-\tau\alpha} \qquad (1)$$

Here, τ refers to time from bolus arrival, K is a scaling constant, and α and β are additional "rate" parameters. The τ in this expression equals $t\text{-}t_0$ where t_0 is the arrival or take-off time.

T2* recovery was computed by calculating the average signal intensity of the last 20 time points as a percentage of the pre-contrast maximum intensity.

Tumor Region of Interest (ROI) Analysis

Once perfusion analysis was completed, ROI analysis was performed. The ROIs were drawn manually using a simple computer pointing device. Four regions of the brain were analyzed in this study: the hemisphere containing the tumor, the contralateral hemi-

sphere, an ROI encompassing the tumor, and an identical region containing healthy tissue, preferably gray and/or white matter, from the uninvolved hemisphere. The hemispheric regions were outlined on the echo-planar perfusion images. The tumor ROIs were drawn on the T1-weighted post-contrast images. An identical area was outlined in the contralateral area of the brain for baseline comparison and statistical evaluation of kinetic parameters. Care was taken to not include the ventricles and bone in the tumor and contralateral regions of interest. These regions were used for analysis of the functional data and to generate relative CBV and CBF maps for each slice through the tumor. Normalized ratios were determined for relative CBV and CBF by taking the mean of the slices divided by the contralateral hemisphere or contralateral ROI.

Statistical Analysis

Statistical analysis was performed using SAS (SAS Institute, Cary, NC). A 99% confidence interval was used to determine cutoff thresholds. A one sample t-test determined the significance of relative CBV and CBF for ROI and hemispheric analyses. A Student's t-test was performed to compare relative CBV and CBF indices of patients with documented clinical responses versus those with progressive disease.

RESULTS

Demographics of the Multi-Institution Trial

The imaging studies analyzed in this report were performed as a component of the NABTT 9911 clinical trial. A total of four institutions were involved in the current phase I trial and are listed in Table 1. Listed in Table 2 are the trial test subjects and their clinical diagnosis.

Data Quality and Reliability

The temporal characteristics of a typical contrast-enhanced perfusion study indicating the MR induced susceptibility drop, the minimum signal intensity time, the signal full-width at half-minimum (FWHMin), and T2* recovery are demonstrated in Fig. 1a. All the data sets were inspected with respect to multiple measures of perfusion reliability. These included the susceptibility characteristics and goodness of the gamma variate fit. Statistical thresholds were computed for these measures. Individual measurements are shown in Fig. 2. The goodness of the gamma variate fit was chosen as a measure of the perfusion analysis efficiency. The FWHMin, minimum signal intensity time and T2* recovery were selected as they reflect the full physical behavior of the MR signal recovery after the susceptibility induced drop.

Table 1
EMD 121974 Multi-Institution Phase I Trial Site Breakdown

Institution	No. of Patients	No. of perfusion studies
University of Alabama at Birmingham (UAB)	18	49
Henry Ford Hospital (HFH)	11	16
Massachusetts General Hospital (MGH)	5	5
Emory University (EMU)	2	2

Table 2
NABTT 9911 Demographics

Patient No.	Dose level	Number of studies	Test site	Clinical diagnosis
1	1	4	UAB	Glioblastoma Multiforme
2	1	2	UAB	Glioblastoma Multiforme
3	1	3	UAB	Anaplastic Astrocytoma
4	1	6	UAB	Glioblastoma Multiforme
5	1	2	UAB	Anaplastic Astrocytoma
6	1	2	UAB	Glioblastoma Multiforme
7	2	2	UAB	Glioblastoma Multiforme
8	2	1	HFH	Anaplastic Oligodendroglioma
9	2	3	UAB	Anaplastic Astrocytoma
10	2	1	HFH	Anaplastic Astrocytoma
11	2	2	UAB	Glioblastoma Multiforme
12	2	2	UAB	Glioblastoma Multiforme
13	2	3	HFH	Glioblastoma Multiforme
14	3	1	HFH	Glioblastoma Multiforme
15	3	2	HFH	Glioblastoma Multiforme
16	3	5	UAB	Anaplastic Astrocytoma
17	3	1	EMU	Glioblastoma Multiforme
18	3	5	UAB	Glioblastoma Multiforme
19	3	1	UAB	Mixed Glioma
20	4	1	EMU	Glioblastoma Multiforme
21	4	1	MGH	Glioblastoma Multiforme
22	4	1	MGH	Anaplastic Astrocytoma
23	4	1	MGH	Anaplastic Astrocytoma
24	4	2	UAB	Glioblastoma Multiforme
25	4	2	HFH	Glioblastoma Multiforme
26	5	1	HFH	Glioblastoma Multiforme
27	5	2	UAB	Glioblastoma Multiforme
28	5	2	HFH	Anaplastic Astrocytoma
29	5	1	MGH	Glioblastoma Multiforme
30	5	1	HFH	Glioblastoma Multiforme
31	6	2	UAB	Glioblastoma Multiforme
32	6	1	HFH	Glioblastoma Multiforme
33	6	1	HFH	Glioblastoma Multiforme
34	6	2	UAB	Anaplastic Astrocytoma
35	6	1	MGH	Mixed Glioma
36	8	2	UAB	Glioblastoma Multiforme

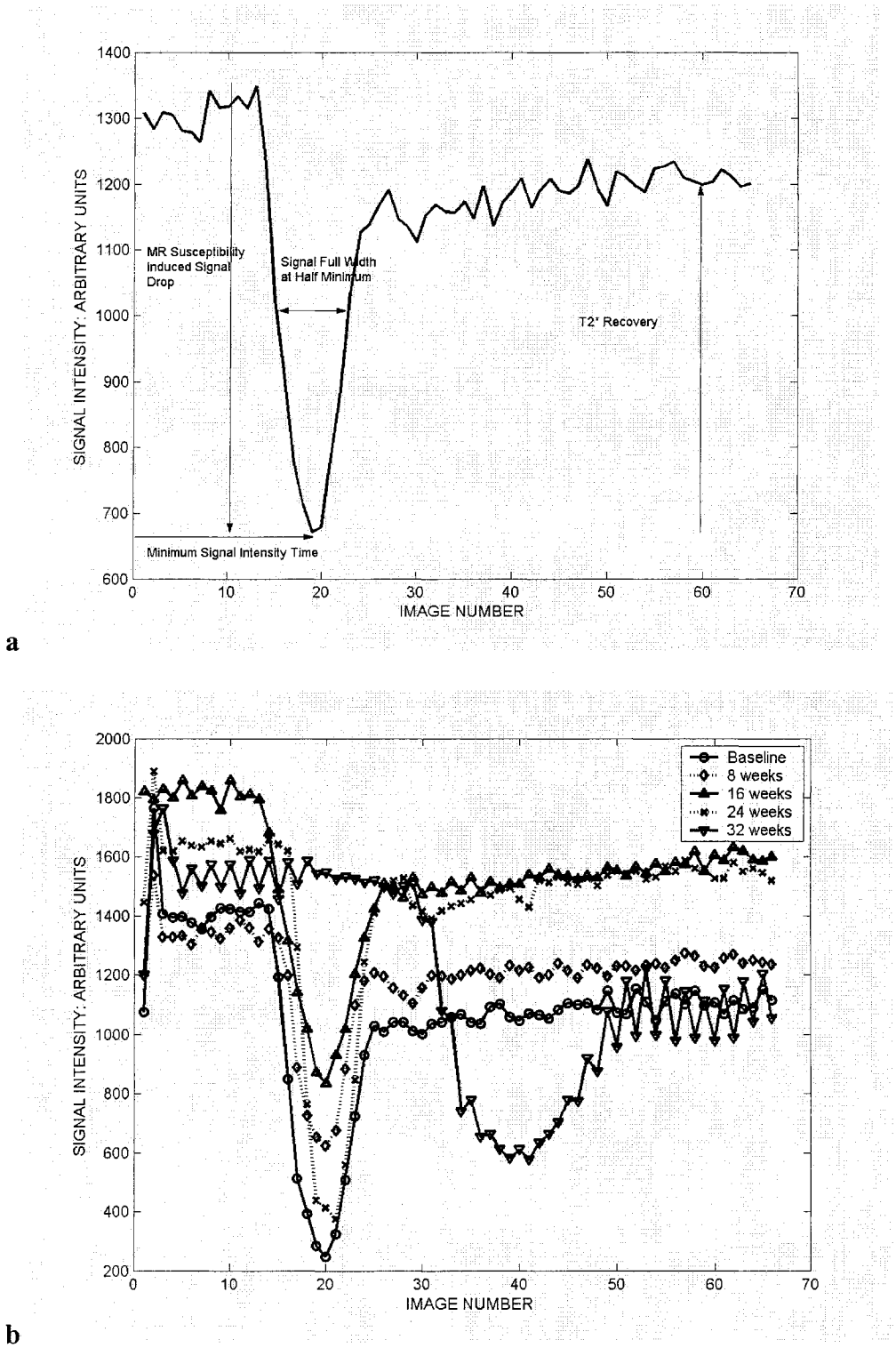

Figure 1. MR Signals. The upper graph (**a**) shows a typical functional time course of a contrast-enhanced perfusion study. The lower graph (**b**) shows pixel time courses from five different perfusion data sets for patient 16. The 32 week study of this patient was discarded because of temporal aberration and a high pixel fit failure percentage.

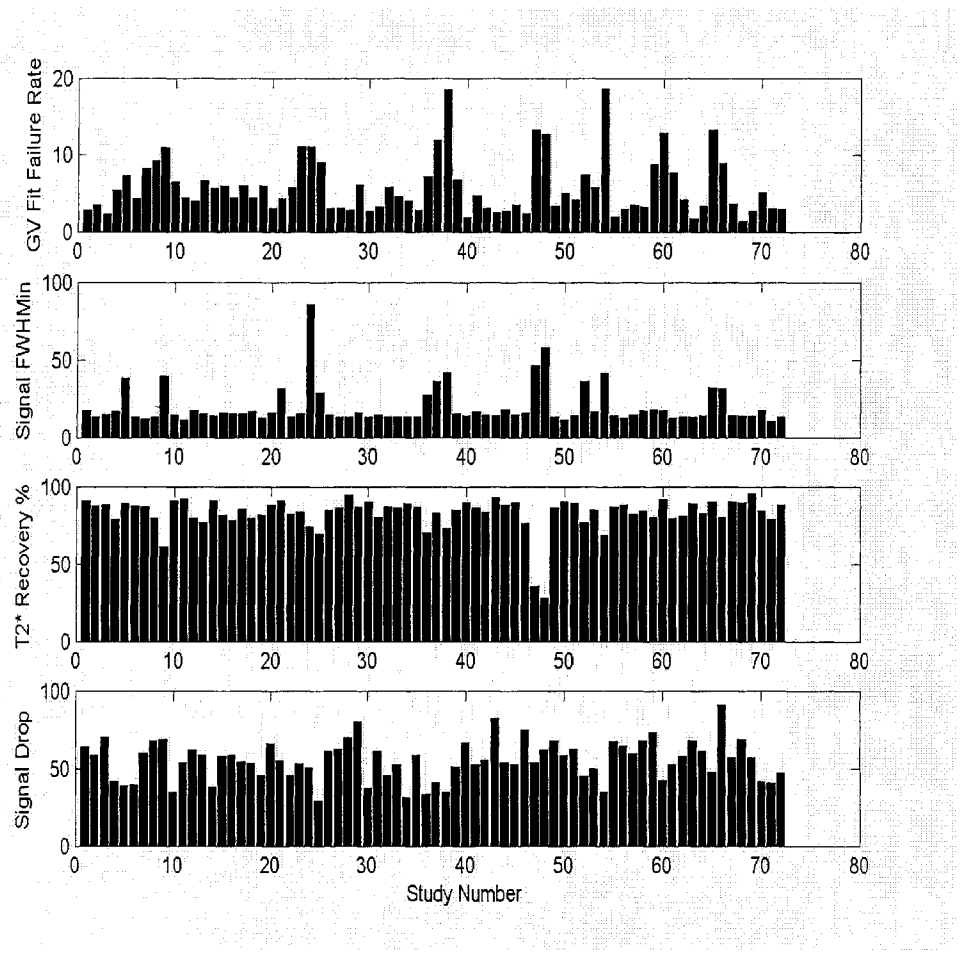

Figure 2. Individual quality measurements for the perfusion data sets. The bar charts represent the four metrics used to statistically standardize the perfusion data sets: The gamma variate fit failure rate, the signal full width at half minimum, the T2* recovery percentage, and MR susceptibility induced signal drop.

The 72 perfusion data sets were analyzed for goodness of the gamma variate fit for all pixels by checking the values of α and β. A pixel was identified as a poor fit if α was negative and β was less than 1, where α and β are the parameters in Eq. 1. Thompson et al (30) showed that these arbitrary distribution parameters determine the shape of the concentration curves. Our data had a mean failure rate of 5.77% (σ = 3.74%). The gamma variate fit failure rates for all the studies are illustrated in Fig. 2. The mean signal FWHMin, T2* recovery and mean MR-induced susceptibility drop were 19.56 seconds (σ = 12.50 seconds), 82.79% (σ = 10.88%), and 55.30% (σ = 12.71%), respectively. The average susceptibility drops were computed by using pixel information from four randomly chosen pixels, one from each quadrant in the images. These pixels were chosen from healthy tissue, i.e., outside the tumor region being studied.

Using a 99% one-sided confidence interval's upper limit, the cut-off thresholds were determined to be 6.91% for gamma variate fit failure rate, 79.48% for the T2* recovery, and 23.35 seconds for the signal FWHMin. Using such a statistical approach allowed us to minimize the T2* effects during the gamma variate fit. All data sets that passed the statistical thresholds for the three above mentioned parameters had a mean minimum signal intensity time of 36.74 seconds (σ = 7.32 seconds), corresponding to maximum contrast agent concentration. Data sets that did not fall within the 99% confidence interval for at least one of the three factors were discarded from further post-processing. Fifty-nine of the data sets passed these quality thresholds. These data sets were then considered for ROI analysis provided they did not have any significant motion or other artifacts.

The importance of statistically determining thresholds to limit data is illustrated in the susceptibility curves of five studies from patient 16 shown in Fig. 1b. Notice that while four studies (baseline, 8-week, 16-week, and 24-week) demonstrated a pattern consistent with the expected theoretical behavior, the fifth study (32-week) shows a temporal aberration in its susceptibility characteristics and was consequently discarded for further post-processing. The temporal shift in signal drop in this study suggests a delayed arrival of the bolus caused by discrepancies in the contrast injection procedure. Data exhibiting such procedural irregularities are hence rejected by our data quality inspection process. The gamma variate pixel fit failure percentages and MR signal statistics for these five studies are tabulated in table 3.

Table 3
Data Quality Inspection Table for Patient No. 16

Study	Percent Fit Failure	Signal Min Time	Signal Full Width at Half Min	Percent Susceptibility drop
Baseline	2.55	30.40	13.54	82.14
8 weeks	2.65	36.10	17.70	53.70
16 weeks	3.45	28.50	14.40	52.26
24 weeks	2.40	30.40	16.11	74.92
32 weeks	12.72	76.00	57.85	61.95

Postprocessing and ROI analysis

Postprocessing was performed on the 59 data sets that met our defined thresholds for quality. ROI analysis of relative CBF and CBV were performed with emphasis on normalized kinetic ratios. The mean ratios for each of these studies are illustrated in Fig. 3. The data represented by diamonds are values for the tumor ROIs while points shown as

squares represent hemispheric data. The dotted and bold lines indicate relative CBV and CBF, respectively.

A one-sample t-test was performed on the normalized relative CBV and CBF ratios. The mean normalized relative CBV ratios for hemispheric regions and tumor ROI were 1.01 (standard error [SE] ± 0.02, $P = 0.55$) and 1.45 (SE ± 0.09, $P < 0.0001$), respectively. The mean normalized relative CBF ratios for hemispheric regions and tumor ROIs were 0.99 (SE ± 0.02, $P = 0.48$) and 1.34 (SE ± 0.07, $P < 0.0001$), respectively. The ROIs represent statistically significant increases of relative CBV and CBF by 43.6% and 35.4%, respectively, when analyzed by tumor defined ROI in recurrent malignant glioma. These increases clearly suggest that localized measurements of kinetic parameters, i.e., over specific ROIs, are of greater value in assessing localized tumor perfusion parameters than hemispheric measurements.

An individual example is illustrated in Fig. 4. The post-contrast T1-weighted image with enhancement at the location of the tumor is shown in Fig. 4a. The average signal across the 65 time points in the functional acquisition that generates the susceptibility curve is shown in Fig. 4b. The normalized kinetic ratios (tumor ROI to contralateral ROI) for the perfusion CBV maps are determined if the data set met threshold values. The bar chart shows four clusters (one for each study, chronologically arranged) each with normalized ratios from seven contiguous anatomic slices. This patient showed a partial clinical response while on this trial. The parametric CBV and CBF maps generated by the perfusion analysis are shown in Fig. 4d and 4e, respectively.

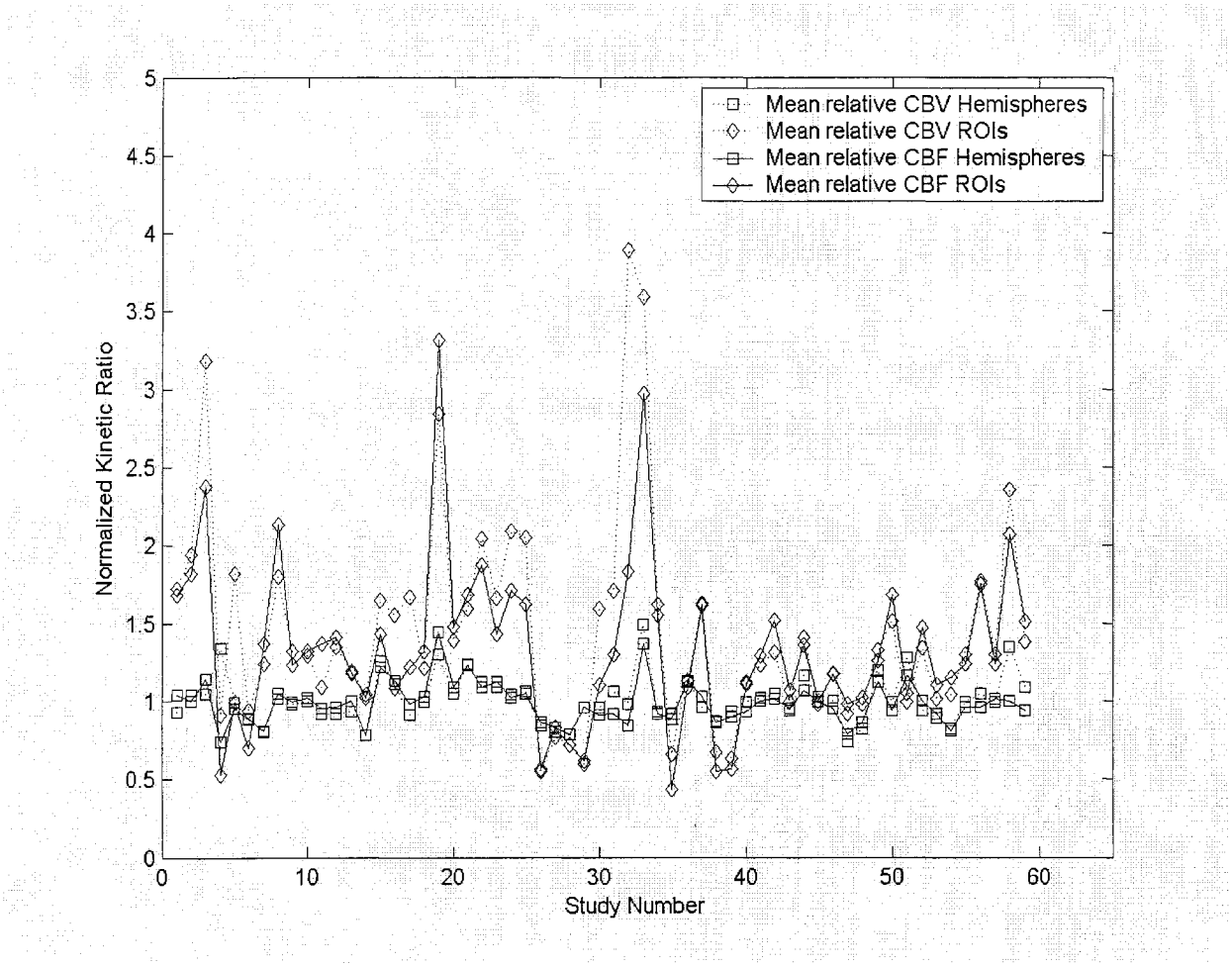

Figure 3. The normalized kinetic parameters for studies in this work showing the relative CBV and relative CBF for hemispheric data and tumor ROIs.

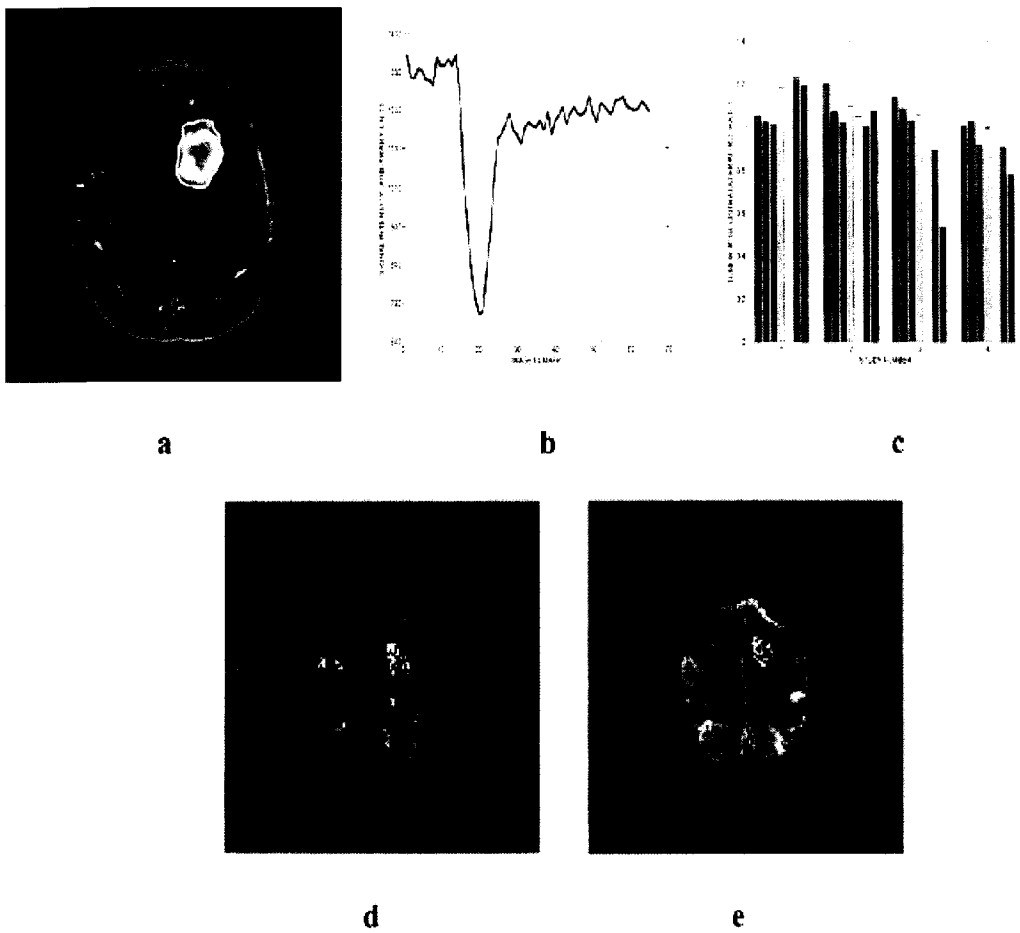

Figure 4. Subject 16, dose level 3. **a:** The T1 post-contrast image indicating the anatomical location of the tumor. **b:** Graph showing the average signal intensity over the functional study. **c:** The normalized CBV values for the seven slices over four studies (Studies were eight weeks apart. **d:** The perfusion CBV map. **e:** The perfusion CBF map. This patient showed a partial clinical response to the angiogenesis inhibitor. Note: a,b,d, and e are from the baseline study.

In this trial the patient response criteria was defined as follows: 1) complete response (CR), complete disappearance of the entire tumor on MRI images, off glucocorticoids, with a stable or improving neurologic examination for at least four weeks; 2) partial response (PR), $\geq$ 50% reduction in tumor size in volumetric MRI studies, on a stable or decreasing dose of glucocorticoids, with a stable or improving neurologic exam for at least four weeks; 3) progressive disease (PD), progressive neurologic abnormalities not explained by causes unrelated to tumor progression, or $\geq$ 25% increase in MR image tumor volume; and 4) stable disease (SD), a patient whose clinical status and MRI volumetrics did not meet the criteria for either PR or PD.

In order to correlate the changes in relative CBV and CBF with the clinical response, the normalized kinetic ratios were tracked longitudinally for patients with multiple perfusion studies. We compared patients with PD with those that had any kind of clinical response (CR + PR + SD = six cases) as well as PD with stable response. We tested changes in relative CBV and CBF by measuring the maximal and minimal differences with respect to the pre-treatment baseline scan. For patients with only two studies, the maximal and minimal differences would be the same. For statistical analysis, we utilized the minimal difference as it is a more rigorous value and less susceptible to bias. The mean changes from baseline are summarized in Table 4. When comparing stable patients and those with PD, the difference between CBV changes is 0.12 ($P = 0.08$) and difference between CBF changes is 0.31 ($P = 0.009$). When comparing PD patients and those that exhibited any response, the difference between CBV changes is 0.24 ($P = 0.08$) and difference between CBF changes is 0.38 ($P = 0.004$). These suggest that the change in relative CBF is the most significant statistical metric for differentiating between patients' clinical responses.

Table 4
Change in CBV and CBF: Comparison of Patients by Clinical Response

Parameter	Clinical response	Mean	Standard error	P-value
CBV	Stable	-0.07	0.03	0.08
	Progression	+0.05	0.05	
CBF	Stable	-0.08	0.04	0.009
	Progression	+0.23	0.07	
CBV	All Response	-0.19	0.08	0.08
	Progression	+0.05	0.05	
CBF	All Response	-0.15	0.05	0.004
	Progression	+0.23	0.07	

Radiographic return to normalcy was observed by tracking the CBF and CBV of patients that demonstrated a clinical response to anti-angiogenic therapy. In addition, patients with documented clinical progression demonstrated increases in the relative CBV and/or CBF. We illustrate four such cases that are summarized in table 5. Patient 4 showed an 8% and 15% decrease in relative CBV and CBF, respectively, from baseline to most recent study. This patient exhibited a stable clinical response. Patient 16 had a 28% drop in CBV and 18% drop in CBF from baseline to most recent study, and clinically showed a PR. Patient 36 showed a 35% and 27% decrease in relative CBV and CBF, respectively, and a complete clinical response. Patient 2 had PD by clinical criteria and a 22% increase in relative CBF.

DISCUSSION

Malignant brain tumors are characterized histologically as very heterogeneous tumors with areas of intense tumor proliferation, neovascularization, and regions of tu-

Table 5
Kinetic Parameters in Patients with Clinical Response to EMD 121974

Study	Patient # 2 Progressive Disease		Patient # 4 Stable Response		Patient # 16 Partial Response		Patient # 36 Complete Response	
	CBV	CBF	CBV	CBF	CBV	CBF	CBV	CBF
Baseline	1.33	1.29	1.08	1.19	1.18	1.19	1.37	1.31
+8 weeks	1.24	1.57	1.18	1.21	1.07	1.16	0.88	0.95
+16 weeks	-	-	1.06	1.13	0.85	0.95	-	-
+24 weeks	-	-	1.07	1.29	0.84	0.97	-	-
+32 weeks	-	-	1.14	1.10	-	-	-	-
+40 weeks	-	-	0.99	1.01	-	-	-	-

mor necrosis (31). The process of tumor-associated vascular proliferation or angiogenesis is believed to be essential for malignant progression (1-3). The molecular steps important for glioma angiogenesis are being elucidated resulting in therapeutic opportunities directed toward this process. The assessment of anti-angiogenic agents in early phase clinical trials has provided unique challenges. The traditional early phase clinical trial design has relied on the development of toxicity to define doses for further efficacy testing. For anti-angiogenic agents, toxicity may be mild and doses associated with toxicity may not necessarily be those associated with biological activity. As a result, clinical investigation with this class of agents may best be served by determining the optimal biological dose (OBD) as opposed to the maximum tolerated dose (MTD). The determination of an OBD would require, as a gold standard, the quantitation of a molecular target or phenotypic change in order to be valid. This validation typically requires obtaining tissue from patients before treatment and at various time points during treatment. This is

not possible with primary brain cancer for several reasons including risk, expense, and biopsy bias. The utilization of non-invasive imaging methodologies like DSC-MRI to assess tumor associated angiogenesis is thus essential for the advancement of novel therapies. Their validation will ultimately require correlation with clinical outcomes that will be possible once the phase I trials are complete.

To utilize noninvasive imaging methods in multi-institution clinical trials, we must first define the requirements of quality and methods for the central analysis of such data sets. The extraction of information on perfusion parameters such as CBV and CBF from DSC-MRI studies and the comparison of this information from one patient to another, from one institution to another, or from one point in time to another require a method to determine if a study meets certain criteria. The susceptibility curve from which perfusion data is extracted is subject to not only differences in the tissue microvascular environment but also to technical factors such as contrast injection rate, contrast concentration, and MR sequence parameters as well as patient factors such as cardiovascular parameters. The standardization of technical and acquisition sequence factors is a clear step in quality control. However, this alone is inadequate for the comparison of perfusion values across institutions and even longitudinally within the same patient. Malignant gliomas are extremely heterogeneous both at the histological and imaging levels. The utility of small ROIs (several pixels) placed in various regions of the tumor will not allow an unbiased evaluation of relative CBV and CBF in the setting of an anti-angiogenic trial. We recommend the use of a ROI, defined on the basis of the complete tumor cross-section, in the post-contrast T1 images.

An issue that merited study was the choice of imaging sequence for our data acquisition. The gradient recalled EPI sequence with interleaved acquisition was chosen for acquiring functional perfusion data. Gradient-echo (GE) EPI and spin-echo (SE) EPI have shown different sensitivities to vessel size, indicating a variation in relative CBVs based on different tumor sizes and grades. GE-EPI and SE-EPI techniques were compared for detecting low- vs. high-grade gliomas and the GE-EPI technique seemed more useful for detecting low- vs high-grade gliomas than the SE-EPI technique (32). In a similar study comparing echo-planar sequences for perfusion-weighted MRI based on image quality, artifacts, signal-to-noise ratio (SNR), and signal attenuation to noise ratio, it was shown that at lower field strengths (2.35 T and less), GRE-EPI sequences are best suited for perfusion studies because they have the highest SNR and T2* sensitivity (33).

Malignant gliomas characteristically have disruption of the blood-brain barrier resulting in the extravasation (34) of gadolinium-based contrast agents into the interstitial space. This may have unwanted effects leading to the underestimation of the CBV and/or CBF. These include both T1 and T2* effects. The T1 effect caused by contrast extravasation is seen as a rise in the signal intensity above baseline after the initial drop (35). This is usually overcome by using techniques like limited integration methods. The T2* effects result in an incomplete recovery of the signal-time intensity curve to baseline and, if excessive, may not allow a gamma variate fit of the data to be achieved. The accuracy of gamma variate fitting in the context of similar contrast-enhanced MRI techniques has been documented earlier (36). Several computational models are available to partially correct for such effects but these are computationally demanding. An alternate solution is to administer a small pre-dose of contrast agent to saturate brain tissue and minimize con-

trast agent leakage during the actual perfusion study. The use of statistical thresholds to help define MRI parameters like susceptibility characteristics as well as CBV and CBF computations is one option for enhancing the quality of study results. Of the data sets in our study, 82% (59 out of 72) passed the statistical quality and reliability thresholds. We believe that statistically limiting our data based on susceptibility characteristics and gamma-variate fit failure rate will standardize results across the institutions involved in the trial.

DSC-MRI has been shown to be a useful tool in assessing brain tumor angiogenesis. Perfusion analyses of primary brain tumors have demonstrated abnormal parameters associated with higher grade (WHO grade III and IV) tumors when compared to normal or low grade (WHO I) (6, 31). In addition, in vivo studies using animal xenograft models of human gliomas support elevated perfusion parameters and are able to correlate these findings with histological measures of angiogenesis (25). Our data is the first report of T2* perfusion results for an early phase clinical trial and includes the evaluation of 36 patients with over 70 studies. Malignant gliomas have significantly altered perfusion parameters that vary widely throughout the tumor. The normalization of perfusion results was accomplished by using either the tumor hemisphere to the uninvolved hemisphere or a tumor defined ROI to a contralateral uninvolved ROI. Hemispheric information about perfusion that was easier to define and less time consuming did not lead to significant inferences about perfusion properties either at baseline or over time. The 34% to 42% increase in kinetic indices when using a specific ROI indicate that ROI analysis is useful for studying changes in tumor blood volume/flow. The changes in blood flow and volume merit a detailed statistical analysis and possibly correlation with clinical outcomes of the

patients. This could yield critical information about tumor proliferation or regression non-invasively. The efficacy of angiogenesis inhibitors like EMD 121974 can be gauged by non-invasively measuring local relative CBV and CBF. In select patients who were on angiogenesis inhibitor treatment, significant reductions in the perfusion parameters in surrounding areas of the primary tumor were observed. Patients were imaged before the start of the administration of EMD 121974 and at subsequent intervals of eight weeks. The temporal changes in normalized kinetic indices are suggestive of a slow decrease in blood vessel proliferation in the tumor. The normalized kinetic ratios were tracked over a period of time over several anatomic slices. The ratios for CBV and CBF decreased significantly. The relative CBV ratios decreased 8% to 36% and relative CBF ratios decreased 15% to 28% in select patients that demonstrated a clinical response. In contrast, patients with progressive disease clinically demonstrated increases in these values. The variations in relative CBV and CBF across several anatomic slices indicate that these perfusion indices are very heterogeneous over the tumor volume. This is as suggested by earlier reports on tumor histology although we did not attempt to establish such a correlation in this study. Our results do indicate that in the assessment of anti-angiogenic agents in early phase clinical trials, the definition of the ROI is of critical importance.

The use of DSC-MRI is a viable method for the assessment of perfusion parameters in the evaluation of anti-angiogenic agents. This is confirmed for the measure of relative CBF by a statistically significant correlation with clinical responses. This is suggested for relative CBV that approached significance in our study. As we progress with further clinical evaluations with increased sample size, statistical correlations will be more robust. The present study included patients with recurrent malignant glioma, of

which nine were initially diagnosed as anaplastic astrocytoma (AA, grade III) and 24 as GBM (grade IV). An analysis of relative CBV and CBF did not demonstrate statistically significant differences between GBM and AA. As the patient population eligible for this trial was at recurrence, the lack of a difference may be reflected in the transformation or progression of many of the AA cases to GBM. CBF and CBVmay not distinguish between these two grades of malignant tumors.

Specialized pixel coregistration techniques could help in monitoring the same location of a patient's brain images over a period of time and would potentially present more accurate localized hemodynamics. In the case of patients who showed a clinical response to the angiogenesis inhibitor, functional perfusion MRI studies showed a decrease in normalized ratios of both relative blood volume and flow. The reduction of these ratios shows that these patients had similar hemodynamics in the tumor ROI and in areas of healthy tissue. These ratios typically dropped to 1.00 and below. Ratios below 1.0 are possible effects of radiation necrosis, edema, or surgery. Radiographic response of brain tumor patients using DSC-MRI can thus be used to non-invasively assess patient progress and also the efficacy of the drug provided studies are subjected to rigorous quality evaluations.

In summary, we have used DSC-MRI data from a multi-institution trial to define the requirements for quality and reliability thresholds that permit analyses of perfusion parameters. These parameters are abnormal in malignant gliomas when analyzed with a defined ROI and may be utilized to evaluate the biological activity of anti-angiogenic drugs in efficacy trial testing.

ACKNOWLEDGMENTS

We thank Brad Hershey, Jane Moody and Lisa Scarpace for their help with MR perfusion imaging data transfer and organization. We also thank Dr. George Hunter for his valuable comments. This work was supported by NIH grants R21 CA 091560 and RR00032UABGCRC to L.B.N.

REFERENCES

1. Folkman. J. What is the evidence that tumors are angiogenesis dependent? J Natl Cancer Inst 1990;82:4-6.

2. Hanahan D, Folkman. J. Patterns and emerging mechanisms of the angiogenesis switch during tumorigenesis. Cell 1996;86:353-364.

3. Rak J, Croix BS, Krebel. R. Consequences of angiogenesis for tumor progression, metastasis and cancer therapy. Anticancer Drugs 1995;6:3-18.

4. Brem S, Cotran R, Folkman. J. Tumor Angiogenesis: a quantitative method for histological grading. J Natl Cancer Inst 1972;48:347-356.

5. Goldbrunner RH, Wagner S, Roosen K, Tonn JC. Models for assessment of angiogenesis in gliomas. J Neurooncol 2000;50:53-62.

6. Leon S, Folkerth RD, Black PM. Microvessel density is a prognostic indicator for patients with astroglial brain tumors. Cancer 1995;77:362-372.

7. Abdulrauf SI, Edvardsen K, Ho KL, Yang XY, Rock JP, Rosenblum ML. Vascular endothelial growth factor expression and vascular density as prognostic markers of survival in patients with low-grade astrocytoma. J Neurosurg 1998;88:513-520.

8. Sorenson AG, Reimer P. Cerebral MR perfusion imaging: principles and current applications. Stuttgart: Georg Thieme Verlag; 2000. 152 p.

9. Rempp KA, Brix G, Wenz FRBC, Guckel F, Lorenz WJ. Quantification of regional cerebral blood flow and volume with dynamic susceptibility contrast-enhanced MR imaging. Radiology 1994;193:637-641.

10. Edelman RR, Mattle HP, Atkinson DJ. Cerebral blood flow: assessment with dynamic contrast-enhanced T2*-weighted MR imaging at 1.5 T. Radiology 1990;176:211-220.

11. Albert MS, Huang W, Lee JH, Pathak CS. Susceptitbility changes following bolus injections. Magn Reson Med 1993;29:700-708.

12. Rosen BR, Belliveau JW, Buchbinder BR. Contrast agents and cerebral hemodynamics. Magn Reson Med 1991;19:285-292.

13. Rosen BR, Belliveau JW, Aronen HJ, et al. Susceptibility contrast imaging of cerebral blood volume: human experience. Magn Reson Med 1991;22:293-299.

14. Daldrup H, Shames DM, Wendland M, et al. Correlation of dynamic contrast enhanced magnetic resonance imaging with histological tumor grade: comparison of macromolecular and small-molecular contrast media. Neuroradiology 1998;28:67-78.

15. Pathak AP, Schmainda KM, Ward BD, Linderman JR, Rebro KJ, Greene AS. MR-derived cerebral blood volume maps: issues regarding histological validation and assessment of tumor angiogenesis. Magn Reson Med 2001;46:735-747.

16. Roberts HC, Roberts TP, Bollen AW, Ley S, Brasch RC, Dillon WP. Correlation of microvascular permeability derived from dynamic contrast-enhanced MR imaging with histologic grade and tumor labeling index: a study in human brain tumors. [Comment]. Acad Radiol 2001;8:384-391.

17. Shin JH, Lee HK, Kwun BD, et al. Using relative cerebral blood flow and volume to evaluate the histopathologic grade of cerebral gliomas. Am J Roentgenol 2002;179:783-789.

18. Sugahara T, Korogoi Y, Kochi M, et al. Correlation of MR imaging-determined cerebral blood volume maps with histological and angiographic determination of vascularity of gliomas. Am J Roentgenol 1998;171:1479-1486.

19. Knopp EA, Cha S, Johnson G, et al. Glial neoplasms: dynamic contrast enhanced T2* -weighted MR imaging. Radiology 1999;211:791-798.

20. Provenzale JM, Wang GR, Brenner T, Petrella JR, Sorensen AG. Comparison of permeability in high-grade and low-grade brain tumors using dynamic susceptibility contrast MR imaging. Am J Roentgenol 2002;178:711-716.

21. Port RE, Knopp MV, Brix. G. Dynamic contrast-enhanced MRI using Gd-DTPA: interindividual variability of the arterial input function and consequences for the assessment of kinetics in tumors. Magn Reson Med 2001;45:1030-1038.

22. Uematsu H, Maeda M, Sadato N, et al. Blood volume of gliomas determined by double-echo dynamic perfusion-weighted MR imaging: a preliminary study. AJNR Am J Neuroradiol 2001;22:1915-1919.

23. Ludemann L, Hamm B, Zimmer C. Pharmacokinetic analysis of glioma compartments with dynamic Gd-DTPA-enhanced magnetic resonance imaging. Magn Reson Imaging 2000;18:1201-1214.

24. Jackson A, Kassner A, Annesley-Williams D, Reid H, Zhu XP, Li KL. Abnormalities in the recirculation phase of contrast agent bolus passage in cerebral gliomas: comparison with relative blood volume and tumor grade. [Comment]. AJNR Am J Neuroradiol 2002;23:7-14.

25. Gossman A, Helbich TH, Kuriyama N, et al. Dynamic contrast-enhanced magnetic resonance imaging as a surrogate marker of tumor response to anti-angiogenic therapy in a xenograft model of glioblastoma multiforme. J Magn Reson Imaging 2002;15:233-240.

26. Jackson A, Kassner A, Zhu XP, Li KL. Reproducibility of T2* blood volume and vascular tortuosity maps in cerebral gliomas. J Magn Reson Imaging 2001;14:510-516.

27. Boxerman JL, Hamberg LM, Rosen BR, Weisskofff RM. MR contrast due to intravascular magnetic susceptibility perturbations. Magn Reson Med 1995;34:555-566.

28. Morris ED, Tasciyan TA, VanMeter JW, Maisog JM, Zeffiro TA. Automated determination of the arterial input function for MR perfusion analysis. In: Proceedings of the 8th Annual Meeting of the ISMRM, Denver, 2000.

29. Ostergaard L, Weisskoff RM, Chesler DA, Gyldensted C, Rosen BR. High resolution measurement of cerebral blood flow using intravascular tracer bolus passages. Part I: mathematical approach and statistical analysis. Magn Reson Med 1996;36:715-725.

30. Thompson HK Jr., Starmer CF, Whalen RE, McIntosh HD. Indicator transit time considered as a gamma variate. Circ. Res. 1964; 14:502-515.

31. Burger PC, Scheithauer BW. Tumors of the central nervous system. Washington, D. C.: Armed Forces Institute of Pathology; 1994. 452 p.

32. Sugahara, T, Korogoi Y, Kochi M, Ushio Y, Takahashi M. Perfusion-sensitive MR imaging of gliomas: comparison between gradient-echo and spin-echo echo-planar imaging techniques. AJNR Am J Neuroradiol 2001; 22:1306-1315.

33. Heiland S, Kreibich W, Reith W, et al. Comparison of echo-planar sequences for perfusion-weighted MRI: which is best? Neuroradiology 1998;40:216-221.

34. Essig M, Wenz F, Scholdei R, et al. Dynamic susceptibility contrast-enhanced echo-planar imaging of cerebral gliomas, effect of contrast medium extravasation. Acta Radiol 2002;43:354-359.

35. Wong JC, Provenzale JM, Petrella JR. Perfusion MR imaging of brain neoplasms. AJR Am J Roentgenol 2000;174:1147-1157.

36. Benner T, Heiland S, Erb G, Forsting M, Sartor K. Accuracy of gamma-variate fits to the concentration-time curves from dynamic susceptibility-contrast enhanced MRI. Magn Reson Imaging 1997;15:307-317.

A QUANTITATIVE TECHNIQUE TO ESTIMATE BRAIN TUMOR ANGIOGENESIS AND ITS SPATIAL VARIATION IN VIVO

by

N. SHASTRY AKELLA, DONALD B. TWIEG, AND L. BURT NABORS

In preparation for submission to *Journal of Magnetic Resonance Imaging*

Format adapted for dissertation

ABSTRACT

Purpose: To develop and test a quantitative technique to quantify angiogenesis in brain tumor patients using perfusion and anatomic magnetic resonance (MR) images, and to examine the spatial and longitudinal variation of angiogenesis in vivo.

Materials and Methods: Five patients with clinical diagnoses of glioblastoma multiforme (GBM) were imaged using dynamic susceptibility contrast-enhanced MRI (DSC-MRI). Empirical hemodynamic information such as relative cerebral blood flow (CBF) and relative cerebral blood volume (CBV) were used to estimate angiogenesis. The angiogenesis potential, $\mathcal{A}$, was computed for each pixel. A concentric annular model is presented and used to evaluate the spatial variance of $\mathcal{A}$. Inter-patient data was used to assess the spatio-temporal patterns of hemodynamics in malignant tumors. One patient with a follow-up imaging study was evaluated for longitudinal changes in angiogenic regions.

Results: It is possible to quantify angiogenesis on a pixel-by-pixel basis using hemodynamic indices such as CBF, CBV, and T2* recovery. All five patients demonstrated a significant increase in vasculature and blood flow at distances of 60%-95% of their tumor radii, and central necrotic areas consistent with the histopathology of malignant brain cancer. The patient studied for longitudinal changes demonstrated an outward growth in angiogenic areas.

Conclusions: Malignant brain tumors have remarkable similarity in the spatial distribution of their angio-architecture, as assessed by perfusion MRI. It is possible to quantitatively estimate brain tumor angiogenesis in vivo and study its spatial variance using a model such as the one proposed.

INTRODUCTION

Ever since research has shown that tumor growth is angiogenesis dependent (1), the understanding, regulating, and monitoring of tumor vasculature is developing into a clinical strategy for tumor therapy and management. Non-invasive advances of techniques such as perfusion magnetic resonance imaging (MRI) are now allowing the quantitative interrogation of cerebral hemodynamics, thereby permitting increasingly accurate measurements of tumor metabolism end-points. Several groups have focused on studying mechanisms of tumor vascularization, including analyses of the growth factors and receptors involved. These efforts have resulted in various approaches for anti-angiogenic treatment of brain tumors (2). Many of the current techniques that are used to study tumor vascularization are invasive and fail to delineate the spatial heterogeneity inherent to malignant gliomas.

In this work, we attempt to mathematically predict the likelihood of an image pixel being angiogenic based on its characteristics, i.e., anatomy, blood flow, volume and other T2*-susceptibility physics-dependent parameters. The model suggested here is easily extended to other indices such as diffusion and spectral/biochemical characteristics of the pixel, whence greater accuracy will be possible. Our approach is strictly a post-processing technique (3) and can be performed in conjunction with routine dynamic susceptibility contrast-enhanced MRI (DSC-MRI) studies on clinical scanners used routinely to assess cerebral hemodynamics.

Blood supply characteristics can be detected in vivo based on the susceptibility physics of paramagnetic contrast agents using fast echo-planar MR imaging techniques with a temporal resolution of 1-2 seconds. Parametric maps of hemodynamic parameters such as relative cerebral blood volume (CBV), relative cerebral blood flow (CBF) and

mean transit time (MTT) may be obtained from perfusion imaging data-sets. These maps have been shown to aid the diagnoses of infarcts, tumor, radiation necrosis, etc. (4). The functional data sets also contain hemodynamic information such as mean signal drop, bolus arrival time, and T2* recovery.

Parametric maps do however have a drawback in that they do not fully present the spatio-temporal information of the cerebral hemodynamics. Because it is difficult to visually incorporate all the information available on the perfusion and parametric images, segmentation of perfusion images is a valuable tool to distinguish tissues with different blood supply patterns. Several groups have considered modeling approaches such as principal component analysis (PCA) (5) and independent component analysis (ICA), and thresholding and Bayesian estimation (6) to separate signal from different tissue compartments of a perfusion data set. Kao et al (6) applied their method to brain perfusion MRI to classify the spatio-temporal characteristics of various brain tissue types in normal human brains. Understanding the hemodynamics in abnormal brain pathology will pave the way for improved therapy planning and management of brain tumors.

Perfusion imaging has also been used to segment gray and white matter in the human brain using time-intensity curves obtained with DSC-MRI (7). It was suggested that such techniques may enable identifications of sub-regions of images with homogenous perfusion dynamics so that better analyses of perfusion parameters would be possible. The approach was also shown to be less sensitive to contamination of input curves with tissue components. This is significant because tumor angiogenesis in human brain tumors is thought to be spatially heterogeneous.

Changes in vascular morphology due to tumor angiogenesis have been studied based on magnetic susceptibility contrast mechanisms (8). It was demonstrated that since

$\Delta R2^*/\Delta R2$ increases with vessel size, the ratio could be used as a measure of average vessel size, thereby distinguishing areas of the brain with patho-physiologically altered vascular proliferation. MR-based vessel size imaging (9) has also been exploited to obtain quantitative measurements of tumor vascularization in rat glioma models. More recently, microvasculature volume measurements using $\Delta R2$ with a super-paramagnetic intravascular agent were shown to correlate with morphometric CBV (10). Such techniques may be used to track angiogenesis-induced changes in vivo.

Image segmentation has been used as a quantitative tool to characterize healthy and pathologic brain tissue. Various techniques have included the use of mean gray level and texture parameters (11), and it has been shown that MR brain images contain features that can reveal discriminant features for tissue classification and image segmentation. Other methods for segmenting brain MR images have included approaches such as artificial neural networks (12), statistical pattern recognition methods (13), histogram shape analysis (14), and other mathematical techniques to extract cerebrospinal fluid, gray matter, and white matter (15, 16). The spatio-temporal characteristics of tumor perfusion can be, as shown in our approach, used to "functionally" segment tumors to identify and monitor processes such as angiogenesis.

The extension of perfusion-based segmentation techniques to examining tumor pathology is of immense clinical interest given the gamut of applications that will benefit from information that can be extracted from such postprocessing techniques. There is a relative paucity of literature studying the application of perfusion-based segmentation to brain tumor models, especially the quantitation of patho-physiological processes like tumor angiogenesis. Our model, based on empirical changes in perfusion parameters, represents one of the first attempts to quantify angiogenesis in vivo using MRI.

MATERIALS AND METHODS

MRI

The imaging sequences were run on a 1.5 T clinical scanner (Signa 5.7, GE Medical Systems, Milwaukee, WI). Five patients with clinically diagnosed high-grade malignant gliomas (glioblastoma multiforme, WHO grade IV) were imaged. These patients presented uni-focal lesions that enhanced upon administration of gadolinium-based contrast agents. They were enrolled in clinical trials to test the therapeutic efficacy of the angiogenesis-inhibitor cilengitide (17). Further, none of the five patients demonstrated clinical response to the therapy. The gradient echo echo-planar imaging (GE-EPI) (128 x 128, TR/TE of 1900/65 msec, FOV of 24 cm x 24 cm, 6 mm slices) was used for DSC-MRI acquisitions. The standard dose of the gadolinium based contrast agent was 0.2 mmol/kg of patient body weight. The contrast agent, magnevist (gadopentate dimeglumine, Berlex Laboratories, Seattle, WA), was injected with a power injector at a flow rate of 4.0 mL/sec and an injection delay of 15 sec. Spin echo post-contrast T1-weighted images (512 x 512, TR/TE of 450/10 msec) were acquired after perfusion imaging for anatomic reference. All imaging studies were approved by our hospital committees. One patient (patient 2) was imaged eight weeks after the initial scan to assess the longitudinal changes in angiogenic patterns. The intra-patient data-sets were not coregistered for longitudinal comparisons.

MR Image Analysis and Postprocessing

Postprocessing and perfusion analysis were performed using the MedX software (version 3.4.2, Medical Numerics, Sterling, VA) running on a Sun Blade 1000 workstation (Sun Microsystems, Palo Alto, CA) with the Solaris 8 Operating System. The data

sets were prepared for postprocessing by inspection for quality, masking, and generation of parametric maps. Masking of the functional data was performed to ensure accurate determination of arterial input function (AIF) and to avoid curve-fitting of pixels outside the brain. A two-stage automatic algorithm (18) was used for identifying arterial voxels in the DSC-MRI data and constructing the AIF. The relative CBV maps are determined though gamma variate fitting (19) of the concentration curves and integration. The relative CBF maps are generated from the amplitude of the residue curve that results from deconvolution of the tissue curve via singular value decomposition.

Further image analyses were then performed using custom-written programs in MATLAB (The Mathworks Inc., Natick, MA). In addition to the relative CBV and CBF parametric maps, we compute the T2* recovery for each pixel. This is done by calculating the difference between the precontrast signal and the average of the last 20 time-points in the DSC-MRI series.

Parameters for angiogenesis quantification

The imaging-based parameters used in perfusion based studies of brain tumors have typically included relative CBV and CBF. Both of these are presumably elevated in angiogenic areas with blood vessels. We include the T2* recovery as a parameter that reflects the leakiness of the vessel and is, hence, indicative of angiogenesis. The local relative CBV, CBF, and T2* recovery were measured in the patient population in four arbitrarily positioned 25 pixel square regions of interest (ROIs).

Based on empirical observations, we model angiogenesis as follows:

$$\mathcal{A} \alpha \, k_1 \cdot f_1(V) \tag{1}$$

$$\mathcal{A} \alpha \, k_2 \cdot f_2(F) \tag{2}$$

$$\mathcal{A} \propto k_3 / f_3(T2^*_{rec}) \quad (3)$$

where $\mathcal{A}$ is the "angiogenesis potential," V is the relative CBV, F is the relative CBF, $T2^*_{rec}$ is the T2* recovery computed from the signal time curve of the perfusion study, and k_1, k_2, and k_3 are arbitrary constants. We are assuming that V and F vary linearly with $\mathcal{A}$, and that T2* recovery has an inverse linear relationship with $\mathcal{A}$. Eq. [1-3] are combined, yielding

$$\mathcal{A} = k \cdot V \cdot F / T2^*_{rec} \quad (4)$$

This formalism is used to compute $\mathcal{A}$ on a pixel-by-pixel basis, and the maps are overlaid onto the high-resolution post-contrast T_1-weighted images. Values of $\mathcal{A}$ reported are relative, i.e., absolute $\mathcal{A}$ divided by the maximum $\mathcal{A}$ for a particular image. Flow, volume, and T2* recovery are weighted equally, resulting in a value of k = 1 being used in our computations reported in this work.

Concentric Annular Model of Angiogenesis Quantification

The next step was to investigate the spatial variance of angiogenesis in regions of the patients' brains affected by tumors. The tumor enhancing area was outlined on the post-contrast T1-weighted images and the centroid (planar center of mass) of the tumor was determined. The equivalent tumor radius, $\mathbf{r}_{tum}$, was computed by dividing the equivalent diameter of the ellipse bounding the enhancement area by two. Pixels were classified into concentric annular regions of increasing radii based on their Euclidean distance from the tumor centroid, as shown in Fig. 1. Mean $\mathcal{A}$, V, F, and $T2^*_{rec}$ were computed for each annular region. A reference ROI was placed in the uninvolved hemisphere of the brain

and similar calculations were performed for assessing the parameters in healthy brain tissue.

To reconcile the differing spatial resolutions of the anatomic images and the DSC-MRI perfusion series, the resulting $\mathcal{A}$ maps were resized to be superimposed on 512 x 512 post-contrast T1-weighted images. Nearest neighbor interpolation was performed to up-sample the 128 x 128 maps generated by our programs.

RESULTS

The values of CBV and CBF changes in tumor fringes compared to healthy tissue, averaged over four ROIs in the five patients, are shown in table 1. The mean increase in CBV was 206.4% and the mean increase in CBF was 179.2%. The $T2^*_{rec}$ decreased by an average of 30.4%. Empirical trends of these parameters based on the four ROIs are summarized in Table 2.

Table 1
Perfusion Parameters in Tumor Patients

Patient	CBV	CBF	T2* rec.
1	+360%	+362%	-29%
2	+150%	+82%	-15%
3	+61%	+154%	-26%
4	+356%	+202%	-45%
5	+105%	+96%	-37%

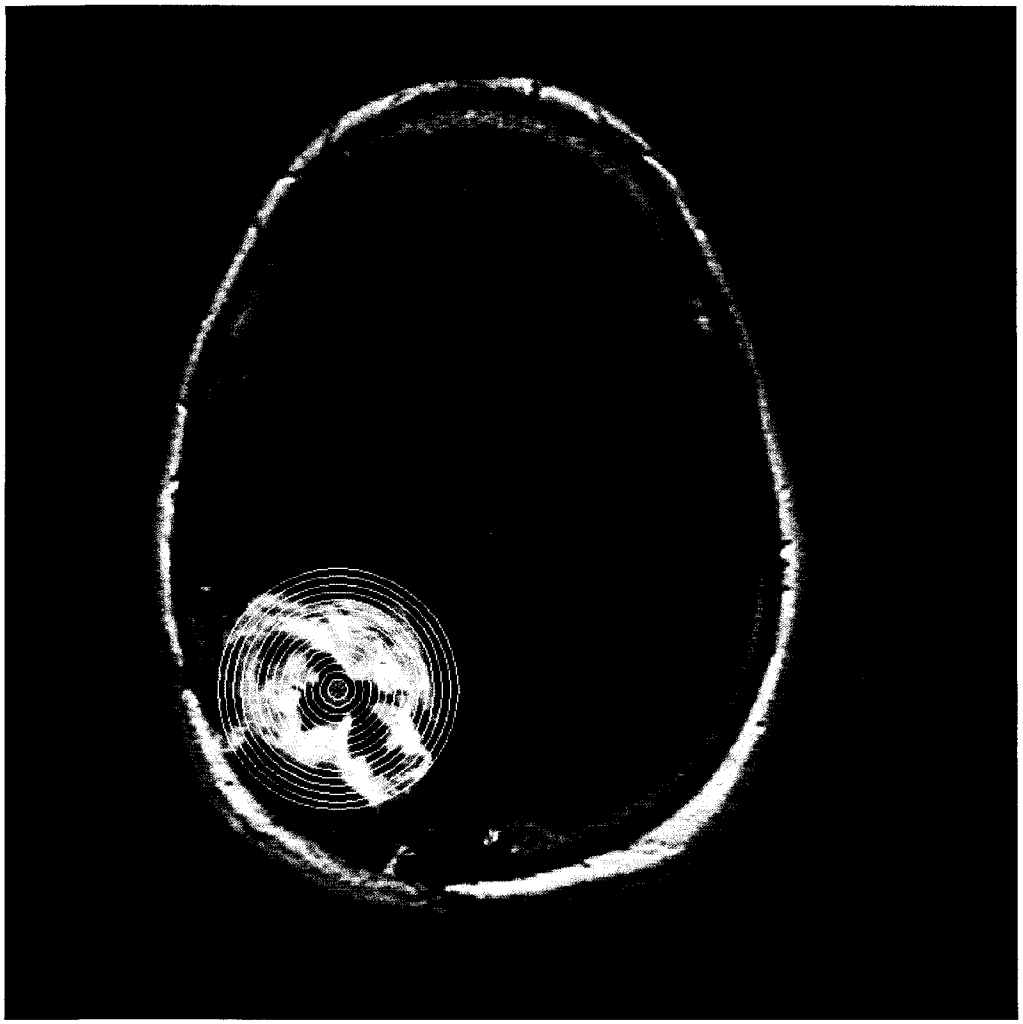

Figure 1. The concentric annular model of angiogenesis quantification. Shown here is the post-contrast T1-weighted image of a subject (patient 1) with a GBM. The red asterisk denotes the centroid of the tumor, while the yellow concentric circles represent the annuli of increasing radii, used to compute various parameters utilized in this study.

Table 2
Changes to Perfusion Parameters during Angiogenesis

Parameter	Behavior in an "angiogenic" pixel, compared to normal brain tissue
CBV (V)	↑ Higher blood volume because of increased vasculature
CBF (F)	↑ Higher blood flow because of increased vasculature
T2* recovery ($T2^*_{rec}$)	↓ Recovery is lower because of vessel leakiness, inherent to high-grade malignant tumors

Patient 1 presented with a GBM, representative of the patient population studied in this work. Figure 2 shows the angiogenesis potential, $\mathcal{A}$, computed by our technique. Results of application of the concentric annular model are illustrated in Fig. 3. The cumulative CBV, CBF, and $T2^*_{rec}$ are shown as functions of distance from the tumor centroid. The dotted lines represent values of the same parameters from a contralateral area of the brain with healthy tissue.

Angiogenesis potential maps from the four other patients are presented in Fig. 4. Note the similarity in the angiogenic pixel pattern, with a majority of those pixels nearer the enhancing tumor margins rather than the center. The spatial characteristics of the five patients are presented in Table 3. The $\mathcal{A}$ values for all five patients are show in Fig. 5 as a function of their distance from their respective tumor centroids.

Table 3
Spatial Characteristics of Brain Tumors

Patient	r_{tum} (pixels)	Peak $\mathcal{A}$ distance ($< r_{tum}$)	Increased $\mathcal{A}$ beyond tumor radius
1	68	60%	No
2	45	74%	Yes
3	53	96%	Yes
4	65	58%	Yes
5	38	61%	Yes

One patient (no. 2) was followed-up after 8 weeks to assess the longitudinal changes in angiogenic patterns. The angiogenesis potential maps from the two studies are presented in Fig. 6, and the findings are tabulated in Table 4.

Table 4
Spatial Characteristics of Patient 2: Longitudinal Changes

Study date	r_{tum} (pixels)	Peak $\mathcal{A}$ distance ($< r_{tum}$)	Tumor enhancement ROI (in pixels)
Baseline	45	74%	2697
+8 weeks	63	97%	3002

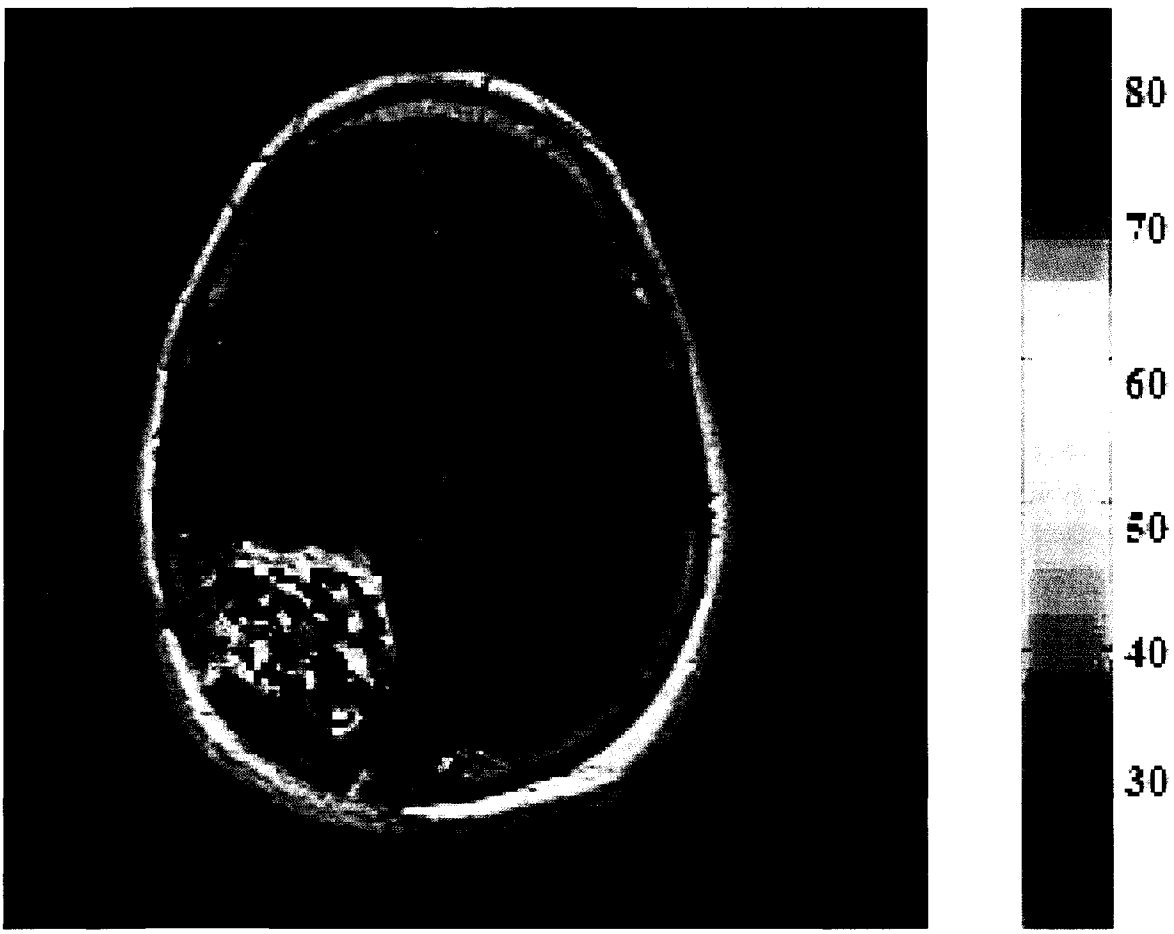

Figure 2. Patient 1: The $\mathcal{A}$ map overlaid on a post-contrast T1-weighted image.

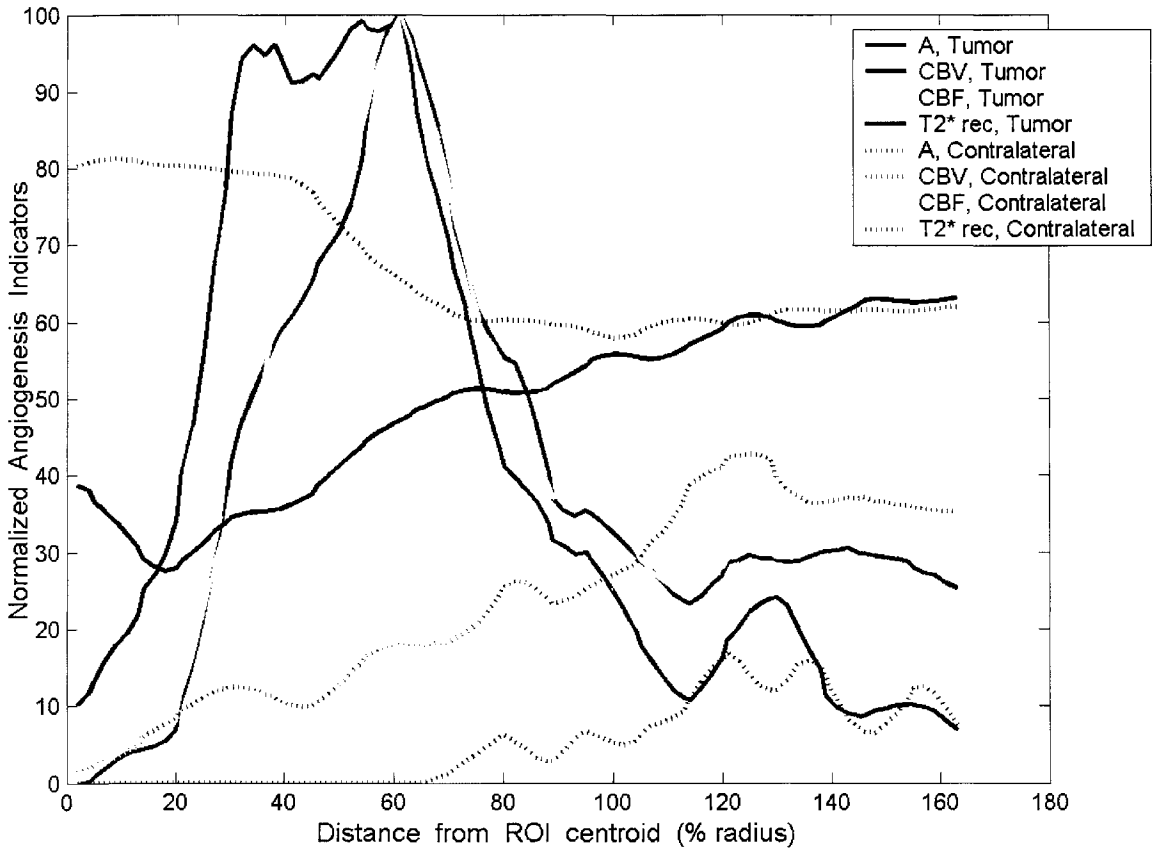

Figure 3. Patient 1: Spatial variation of angiogenesis potential and other perfusion imaging parameters. Illustrated here are the normalized plots of $\mathcal{A}$ and other indices as functions of distance from tumor centroid. Data were computed using the concentric annular model.

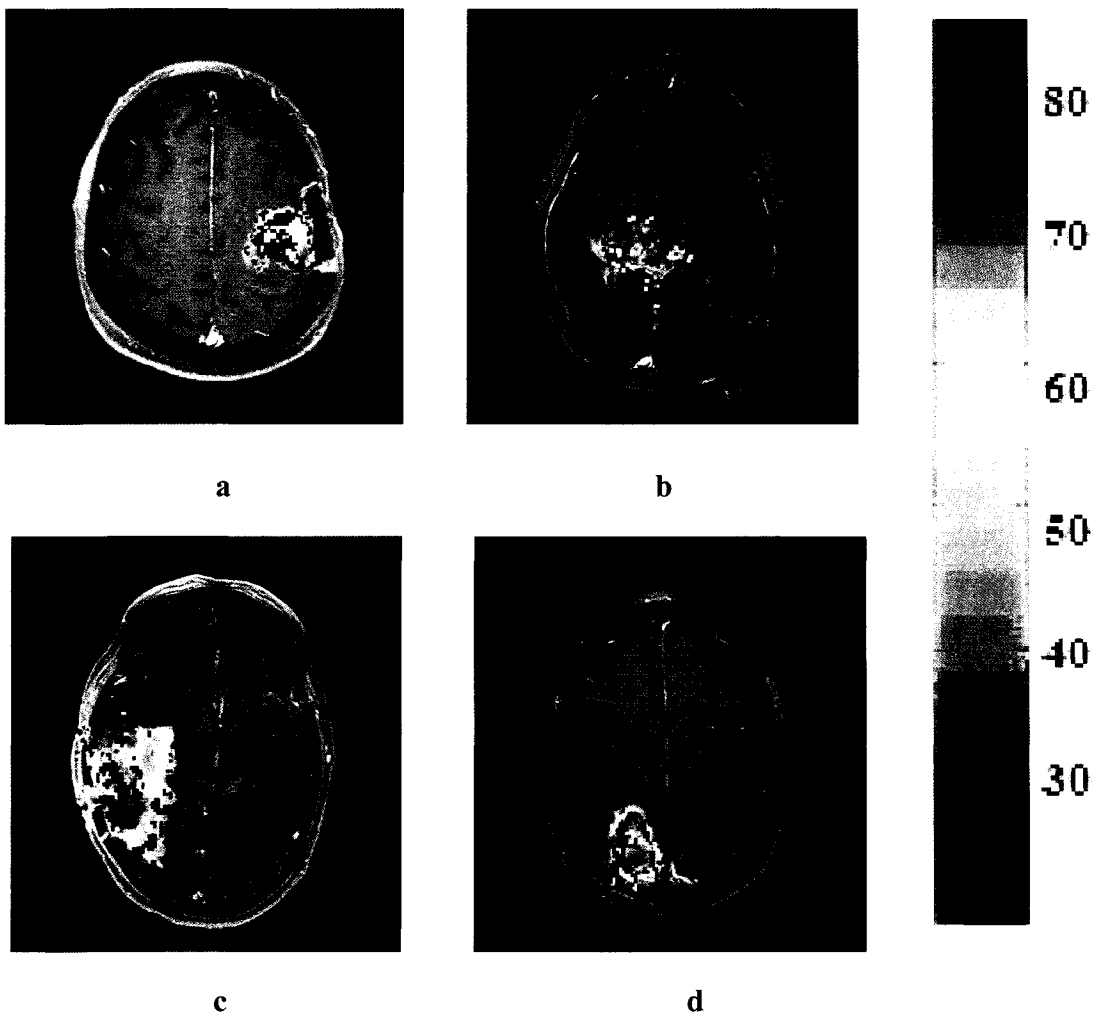

Figure 4. Angiogenesis potential maps of patients. Patients (**a:**2, **b:**3, **c:**4, **d:**5) overlaid onto respective post-contrast T1-weighted images. The tumor centroid in each case is represented by a red asterisk, in the center of the enhancing area.

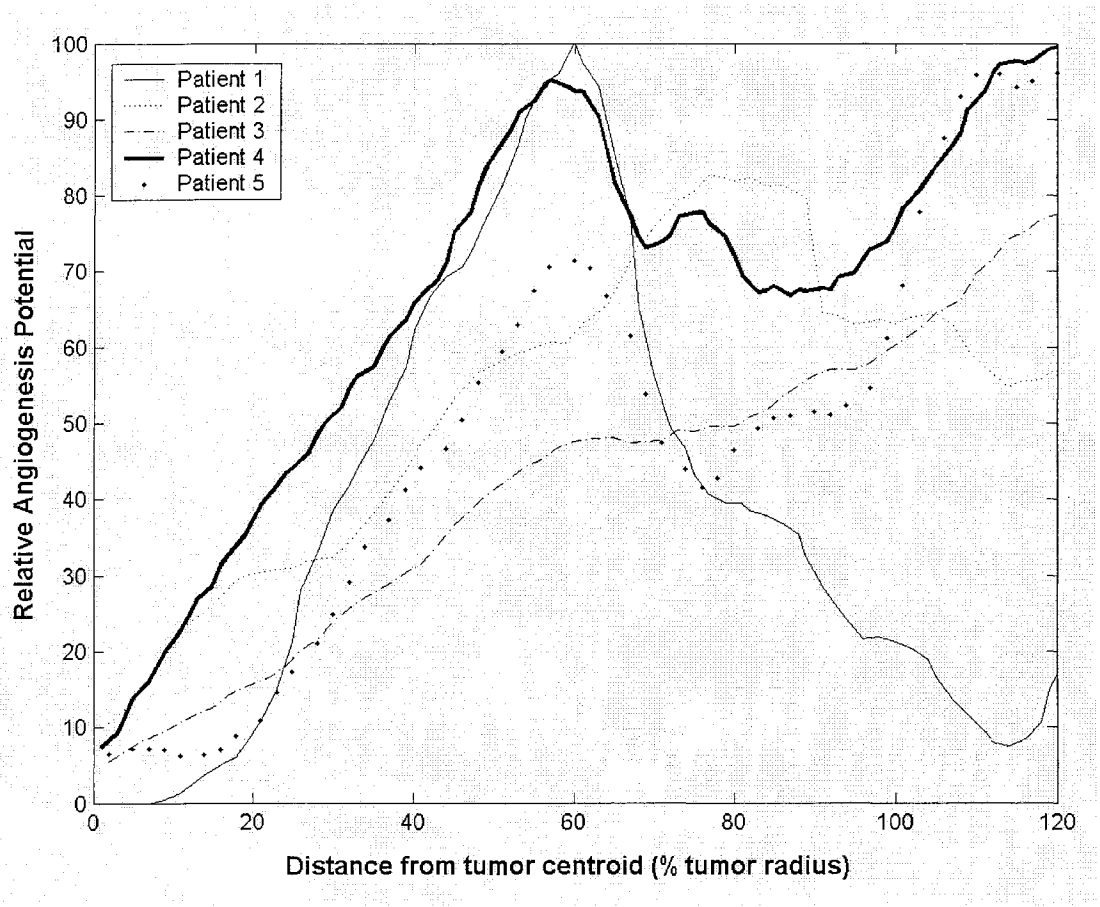

Figure 5. Angiogenesis potential values as a function of distance from tumor centroid for all five patients. The horizontal axis represents distance from the tumor centroid as a percentage of tumor radii. The vertical axis represents relative $\mathcal{A}$ value (absolute value/maximum $\mathcal{A}$ value for patient).

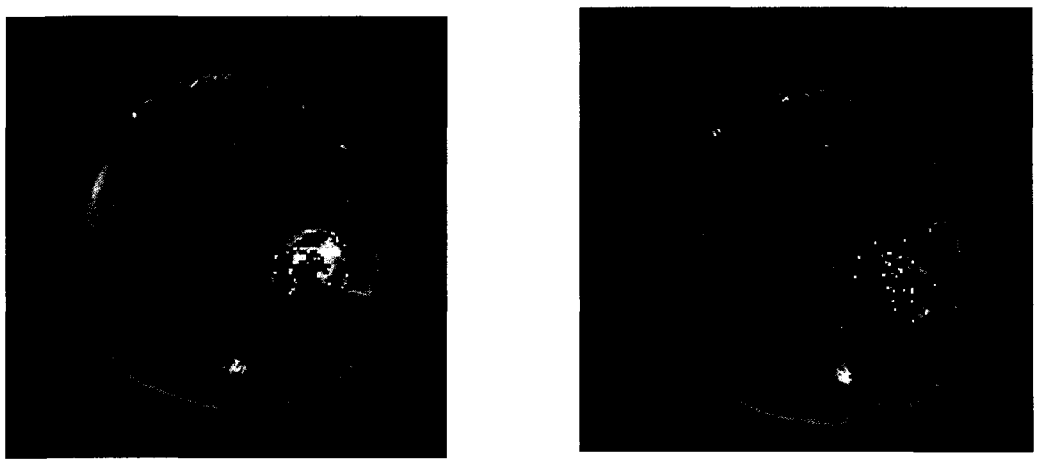

a b

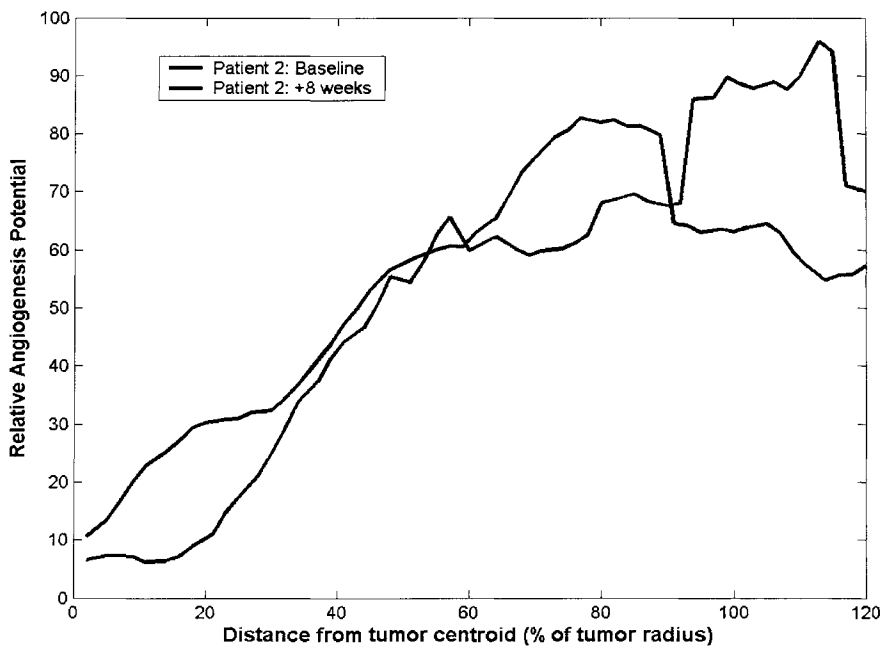

c

Figure 6. Patient 2: Longitudinal changes in angiogenesis. Shown above are the angiogenesis potential maps at (**a**) baseline, and, (**b**) +8 weeks. The longitudinal spatial variation computed using our model is illustrated in (**c**).

DISCUSSION

The radiological assessment of malignant brain tumors using MRI has traditionally relied on the qualitative evaluation of enhancement, mass effect, vasogenic edema, and blood flow and volume. The technique described in this paper is one of the first methods proposed to quantitate angiogenesis based on MR characteristics of parameters such as CBV, CBF, and T2* recovery. These parameters were assumed to have either linear or inverse linear relationships with the proposed angiogenesis potential, $\mathcal{A}$. Other mathematical relationships are being modeled and tested. Corroborating these estimates using histological measures and/or other imaging techniques such as tractography or micro-vessel imaging could improve quantification of angiogenesis using empirical approaches such as the one proposed here. The use of MR relaxation parameters (20) for obtaining high-resolution microvasculature maps could augment mathematical models of angiogenesis.

All patients studied in this work showed similar trends in their angiogenesis potential, $\mathcal{A}$. Beginning with very low values at the center of the tumor, the levels of "angiogenesis" peaked between 60% and 95% of tumor radius, shown in Fig. 5. The low levels of angiogenesis near the tumor center are consistent with a necrotic core, a classic radiological feature of GBM. Some patients showed elevated values of $\mathcal{A}$ even beyond the tumor enhancement boundary, suggesting the presence of neovasculature beyond tumor fringes as defined by contrast enhancement. This, too, is expected in malignant brain cancer, where disease progression is dependent on fringe neovascularization. Our technique also handled healthy brain tissue reliably, not predicting "angiogenic" pixels in contralateral regions of the brain, which were used as reference ROIs.

Given the inherent complexity of the process of angiogenesis, it is critical that vascular morphology be studied in great detail. Tumor aggression and invasion are dependent on the degree of neovascularization. Factors such as stress and hypoxia play significant roles in tumor angiogenesis (21) and add to the heterogeneity of malignant tumors. A quantitative evaluation of angiogenesis is essential for a better understanding of disease progression.

A fundamental confound in susceptibility-based imaging of malignant brain tumor hemodynamics is the leaky blood brain barrier, resulting in extravasation of contrast agent (22). Calculations using a gamma-variate fit often wrongly estimate the blood volume because of the classic over-shoot in signal-time curve due to T1 effects. This may be corrected using postprocessing techniques such as truncating the number of signal-time curve points used or other more sophisticated algorithmic approaches (23), and/or preloading of tissue with a token dose of contrast agent. In our case, the signal-time curve used for the gamma-variate fit was truncated for such compensation. We are currently investigating other approaches to minimize the overestimation of CBV due to the T1 effects.

A potential caveat of the approach suggested here is that the technique assumes every pixel is either angiogenic or not, thereby leaving room for errors caused by partial-volume effects. An increase in the spatial resolution of the DSC-MRI acquisition will, to some degree, compensate for such an error. A more thorough examination of parameters such as mean signal drop and mean transit time could be used to strengthen the model presented, although overcoming the leaky blood brain barrier will continue to be a hurdle in any approach that involves a gadolinium-based exogenous contrast agent. The wrong estimation of hemodynamics caused by contrast agent extravasation could also be over-

come by using either endogenous contrast agents or large particle contrast agents like monocrystalline iron oxide nanocompounds (MIONs) (24). Other quantitative indices such as the apparent diffusion coefficient and fractional anisotropy, which are both computed during postprocessing, could aid in better mapping of vasculature. We have avoided using the bolus arrival time as an indicator of hemodynamics because micro-vessel distribution and vessel tortuosity were not factored into our model, and these are likely to significantly alter the transportation of contrast bolus. MRI-derived CBV maps have been compared with histological measures of micro-vessel density for the evaluation of tumor angiogenesis (25).

Relative CBV and CBF, T2* recovery, and other parameters obtained using the concentric annular model of analysis presented here are consistent with earlier reports of angio-architecture. In large tumors, two distinct patterns have been ascertained (26, 27):

1. A peripheral pattern that involves the continuous development of new micro-vessels and the incorporation of established vessels at the growing edge of the tumor, and
2. A central pattern, in which the paucity of tumor micro-vessels is seen, associated histologically with necrosis.

In patients imaged in this study, blood flow and volume were seen to be concentrated in the fringe areas of the tumor.

Brain tumors are histologically very heterogeneous (28), a fact not always appreciated in non-invasive anatomic and functional imaging techniques such as DSC-MRI. Postprocessing approaches such as ours offer non-invasive methods to not only assess the angiogenesis in vivo, but also provide a measure of the underlying spatial variation. They have the potential to aid biopsy and surgery guidance, but will require reliable image co-

registration algorithms, and are computationally intensive. Appropriate verification of quantitative estimates will have to be made using brain tumor histology and other available techniques. Given the spatial characteristics and heterogeneity of most malignant gliomas, the extension of models such as the one proposed in this work to three spatial dimensions will be required for more comprehensive assessment of growth, metabolism, angiogenesis, and invasion patterns of malignant brain tumors.

A very useful application of our technique is the longitudinal tracking of therapy in patients with brain tumors. As evidenced by the studies on patient 2, it is possible to apply the method to series perfusion studies in an attempt to evaluate the temporal changes in tumor hemodynamics. Patient 2 demonstrated no clinical response to cilengitide therapy. While increased tumor enhancement due to growth was seen in the post-contrast T1 images, quantification of angiogenesis on a pixel-by-pixel basis provided additional information about the vasculature and hemodynamics. In addition to increases in CBV, CBF, and $\mathcal{A}$, patient 2 demonstrated an outward shift of 18 pixels in the enhancing radius, and a corresponding right shift in the $\mathcal{A}$ peak, shown in Fig. 6c. The evolution of tumor hemodynamics over time could very well be a reliable tool in evaluating disease progression, and the rate of change of angiogenesis and quantitative indices such as $\mathcal{A}$ could be utilized in measuring efficacy of anti-angiogenic drugs. Co-registration of intra-patient data sets is of little consequence because the parameters being analyzed are reported with respect to a tumor centroid, computed individually for each study.

More recently, it has been suggested that "normalization" of anti-angiogenic therapy could lead to more efficient anti-cancer therapies (29). This will require frequent and efficient in vivo monitoring of the delicate balance between glioma vascularization, therapeutic interventions and drug uptake, as well as conditions like stress, hypoxia, and

the ever-changing tumor micro-environment. Non-invasive imaging techniques and analyses such as the one presented here provide accurate quantitative estimates of angiogenesis that could be useful in therapy monitoring. Addition of a priori information such as histological and pathological parameters could be used to strengthen quantitative approaches aimed at predicting angiogenesis in vivo. Knowledge of capillary network patterns could also be used to assess the microvascular network in tumors. Based on our results, we strongly feel that the characterization of the "angiotype" of a tumor, first proposed by Hansen-Smith (30), is very critical to our understanding of angiogenesis.

In conclusion, the spatio-temporal information obtained by analyses of DSC-MRI data yields useful information about the vasculature and hemodynamic patterns in malignant brain tumors. It is possible to assign each pixel a likelihood of being angiogenic based on its hemodynamic behavior. The addition of other imaging parameters indicative of tumor microvasculature and direction of blood flow will greatly enhance the clinical utility of such a technique. Development of quantitative indices such as the angiogenesis potential $\mathcal{A}$, presented here, and strengthening of spatio-temporal models for analysis will be very useful tools in monitoring disease progression and therapy efficacy, as well as in surgery and biopsy planning.

ACKNOWLEDGMENTS

We thank Dr. Joel Curé, Jane Moody, and Cleve Crews and the staff of the UAB Department of Radiology, Division of Neuro-radiology, for their help with MRI acquisitions and data transfer. This work was supported by the NIH grant R21 CA 091560 to L.B.N.

REFERENCES

1. Folkman J. Tumor angiogenesis: therapeutic implications. N Engl J Med 1971;285:1182-1186.

2. Goldbrunner RH, Wagner S, Roosen K, Tonn JC. Models for assessment of angiogenesis in gliomas. J Neurooncol 2000;50:53-62.

3. Akella NS, Twieg DB, Nabors LB. Quantitative estimation of angiogenesis in vivo. In: Proceedings of the 13th Annual Meeting of ISMRM, Miami, 2005.

4. Sorenson AG, Tievsky AL, Ostergaard L, Weisskoff RM, Rosen BR. Contrast agents in functional MR imaging. J Magn Reson Imaging 1997;7:47-55.

5. Martel AL, Moody AR, Allder SJ, Delay GS, Morgan PS. Extracting parametric images from dynamic contrast-enhanced MRI studies of the brain using factor analysis. Med Image Anal 2001;5:29-39.

6. Kao YH, Guo WY, Wu YT, et al. Hemodynamic segmentation of MR brain perfusion images using independent component analysis, thresholding, and Bayesian estimation. Magn Reson Med 2003;49:885–894.

7. Wiart M, Rognin N, Berthezene Y, Nighoghossian N, Froment JC, Baskurt A. Perfusion-based segmentation of the human brain using similarity mapping. Magn Reson Med 2001;45:261-268.

8. Dennie J, Mandeville JB, Boxerman JL, Packard SD, Rosen BR, Weisskoff RM. NMR imaging of changes in vascular morphology due to tumor angiogenesis. Magn Reson Med 1998;40:793-799.

9. Tropes I, Lammalle L, Peoc'h M, et al. In vivo assessment of tumoral angiogenesis. Magn Reson Med 2004;51:533-541.

10. Dunn JF, Roche MA, Springnett R, et al. Monitoring angiogenesis in brain using steady-state quantification of delta R2 with MION infusion. Magn Reson Med 2004;51:55-61.

11. Herlidou-Meme S, Sonstans JM, Carsin B, et al. MRI texture analysis on texture test objets, normal brain and intercranial tumors. Magn Reson Imaging 2003;21:989-993.

12. Reddick WE, Glass JO, Cook EN, Elkin TD, Deaton RJ. Automated Segmentation and Classification of Multispectral Magnetic Resonance Images of Brain Using Artificial Neural Networks. IEEE Trans Med Imaging 1997;16:911-918.

13. Andersen AH, Zhang Z, Malcom J. Acison, Gash DM. Automated segmentation of multispectral brain MR images. J Neurosci Methods 2002;122:13-23.

14. Schnack HG, Pol HEH, Barre WFC, Staal WG, Viergever MA, Kahn RS. Technical Note. Automated separation of gray and white matter from MR images of the human brain. Neuroimage 2001;13:230-237.

15. Thaker NA, Jackson A. Mathematical segmentation of grey matter, white matter and cerebral spinal fluid from MR image pairs. Br J Radiol 2001;74:234-242.

16. Kovacevic N, Lobaugh NJ, Bronskill MJ, Levine B, Feinstein A, Black SE. A robust method for extraction and automatic segmentation of brain images. Neuroimage 2002;17:1087-1100.

17. Akella NS, Twieg DB, Mikkelsen T, et al. Assessment of brain tumor angiogenesis inhibitors using perfusion magnetic resonance imaging - quality and analysis results of a Phase I Trial. J Magn Reson Imaging 2004;20: 913-922.

18. Morris ED, Tasciyan TA, VanMeter JW, Maisog JM, Zeffiro TA. Automated determination of the arterial input function for MR perfusion analysis. In: Proceedings of the 8th Annual Meeting of the ISMRM, Denver, CO, 2000; 8:740.

19. Ostergaard L, Weisskoff RM, Chesler DA, Gyldensted C, Rosen BR. High resolution measurement of cerebral blood flow using intravascular tracer bolus passages. Part I: mathematical approach and statistical analysis. Magn Reson Med 1996;36:715-725.

20. Wu EX, Tang H, Jensen JH. High-resolution MR imaging of mouse brain microvasculature using the relaxation rate shift index Q. NMR Biomed 2004;17:507-512.

21. Shweiki D, Neeman M, Itin A, Keshet E. Induction of vascular endothelial growth factor expression by hypoxia and by glucose deficiency in multicell spheroids: implications for tumor angiogenesis. Proc Natl Acad Sci USA 1995;92:768-772.

22. Essig M, Wenz F, Scholdei R, et al. Dynamic susceptibility contrast-enhanced echoplanar imaging of cerebral gliomas, effect of contrast medium extravasation. Acta Radiol 2002;43:354-359.

23. Wong JC, Provenzale JM, Petrella JR. Perfusion MR imaging of brain neoplasms. Am J Roentgenol 2000;174:1147-1157.

24. Shen T, Weissleder R, Papisov M, Bogdonov A Jr., Brady TJ. Monocrystalline iron oxide nanocompounds (MION): physicochemical properties. Magn Reson Med 1993;29:599-604.

25. Pathak AP, Schmainda KM, Ward BD, Linderman JR, Rebro KJ, Greene AS. MR-derived cerebral blood volume maps: issues regarding histological validation and assessment of tumor angiogenesis. Magn Reson Med 2001;46:735-747.

26. Berger MS and Wilson CB. The Gliomas. Philadelphia, PA: W. B. Saunders, 1999. p. 87-106.

27. Deane BR, Lantos PL. The Vasculartures of Experimental Brain Tumours Part 1. A Sequential Light and Electron Microscope Study of Angiogenesis. J Neurol Sci 1981;49:55-66.

28. Burger PC, Scheithauer BW. Tumors of the central nervous system. Washington, D. C.: Armed Forces Institute of Pathology; 1994. 452 p.

29. Jain RK. Normalization of tumor vasculature: an emerging concept in antiangiogenic therapy. Science 2005;307:58-62.

30. Hansen-Smith FM. Capillary network patterning during angiogenesis. Clin Exp Pharmacol Physiol 2000;27:830-835.

CORRELATION OF SPECTRAL AND HEMODYNAMIC INFORMATION IN THE EVALUATION OF BRAIN TUMOR ANGIOGENESIS

by

N. SHASTRY AKELLA, DONALD B. TWIEG,
JAN A. DEN HOLLANDER, AND L. BURT NABORS

In preparation for submission to *Magnetic Resonance Imaging*

Format adapted for dissertation

ABSTRACT

Purpose: To perform perfusion magnetic resonance imaging (MRI) and MR spectroscopic imaging on brain tumor patients and develop a framework to correlate tumor hemodynamics with metabolite concentrations in vivo.

Materials and Methods: Two patients with new clinical diagnoses of primary brain cancer were imaged using dynamic susceptibility contrast-enhanced MRI (DSC-MRI) and 2D chemical shift imaging (CSI). Blood flow and volume measures are computed along with metabolite/spectroscopic images obtained using 2D CSI. These are compared using custom-written MATLAB programs in an attempt to evaluate biochemical changes during tumor angiogenesis in vivo, with respect to three regions: healthy tissue, tumor fringes, and tumor core.

Results: Both patients demonstrated very low cerebral blood flow (CBF) in the tumor core. This corresponded with lowered concentrations of N-acetyl aspartate (NAA) and Choline (Cho). Levels of Cho and CBF were higher in the tumor fringes, but demonstrated variability. A well-resolved lactate/lipid peak was present in one patient.

Conclusions: Spatial variations of parameters that indicate tumor progression, such as CBF and concentration of metabolites like Cho and NAA, correlate with each other. Quantitating these variations will improve our understanding of angiogenesis.

INTRODUCTION

Angiogenesis (i.e., the sprouting of new blood vessels) is believed to be one of the chief mechanisms by which primary malignant brain cancer invades and proliferates. The neovasculature nourishes growing tumors and facilitates tumor expansion beyond 2 mm^3 (1). It has also been shown that tumor phenotypes do not have the normal vascular com-

plex. The interest in anti-angiogenic therapies targeting brain cancer has risen dramatically, aided by the corresponding methodological advances in magnetic resonance imaging (MRI) and spectroscopy, and postprocessing of data acquired therein. Most of the non-invasive evaluations of angiogenesis in the context of brain tumors have relied traditionally on anatomic and perfusion and permeability MRI sequences. These techniques provide anatomic and functional detail respectively, but do not provide biochemical information, which has immense potential to aid in the physiological and biochemical characterization of brain tumor angiogenesis. One way to achieve this is using ^{1}H (proton) MR spectroscopy (MRS) or MR spectroscopic imaging (MRSI). Several reviews have analyzed the role of MRS/MRSI in the evaluation of brain tumors and it is agreed that spectroscopy provides additive information that complements conventional MR imaging (2,3).

In this work, we have attempted to interrogate angiogenesis in vivo, via measurements of metabolite distributions in patients with brain tumors, using spectroscopic imaging sequences available on a clinical MR scanner. We attempt to correlate cerebral metabolite distribution with perfusion measurements such as relative cerebral blood flow (CBF), relative cerebral blood volume (CBV), and a quantitative index of angiogenesis we term the angiogenic potential, $\mathcal{A}$ (4). Our group has reported earlier that relative cerebral blood flow and volume could be used as surrogate markers of angiogenesis in the assessment of response to anti-angiogenic therapy (5). There have been no published reports of application of MRSI techniques to assessment of angiogenesis, a critical aspect of brain tumors, which we investigate in this paper. Absolute patho-physiological correlations will require more rigorous analyses than the one presented here, on larger patient

populations. We attempt to establish the feasibility of a correlative study using a quantitative index of angiogenesis and metabolite maps/spectroscopic images.

Spectroscopy is able to assess tumor vasculature and the microenvironment that sustains the metabolism needed for new blood vessels to form and spread indirectly by evaluating the molecular composition of tissue and the levels of cerebral metabolites that are altered by abnormal pathology. Various techniques involving proton and other nuclei based MR spectroscopy measure the distribution and proportion of molecules within the tissue reflecting factors such as bio-energetics, pH, membrane turnover, and cell oxygenation and death (6).

The combination of conventional volumetric MRI and multivoxel localized MRSI data provides the potential for quantifying variations in tissue morphology and function. Metabolic parameters found most useful in distinguishing tumor from normal and necrotic tissue are levels of choline (Cho) and N-acetyl aspartate (NAA) (7). Levels of creatine (Cre), lactate (Lac), and lipid (Lip) were found to be variable, both in their spatial distribution within individual lesions and in different patients. It is possible to reliably distinguish brain tumors and normal brain tissue based on spectral signatures obtained using MRSI techniques. It has been shown that spectroscopy can also provide useful information about brain tumor type and grade (8). Low levels of NAA are characteristic of high-grade tumors, although the metabolite concentrations differences between glioblastoma multiforme (GBM) and metastases were not statistically significant. In high-grade tumors, the presence of necrosis reduces estimated absolute metabolite concentrations. It is thought that the quantification of lipids may provide a measure of the hypoxic or necrotic fraction. Howe et al. (8) have also observed that metabolic profiles shown by the average ^{1}H spectra for normal white matter, meningiomas, and astrocytomas were very

different, confirming the differences in cell types and metabolism. Other metabolites like alanine, glutamine, and glycine have also been investigated in the context of brain tumor metabolism using MRS techniques.

Techniques for the evaluation of cerebral gliomas using a combination of MRSI, perfusion, and other imaging techniques have been published recently. Relative CBV and metabolite ratios have been shown (9) to increase the sensitivity and positive predictive value when compared with conventional MRI alone. It has been strongly recommended that longitudinal perfusion MRI and spectroscopic data be used in conjunction to predict tumor behavior and patient prognosis. Attempts have been made to correlate kinetic parameters like CBV, the apparent diffusion coefficient (ADC), and metabolite information obtained from proton MRS (10). It was suggested that tumors could be characterized with a high degree of precision using multivoxel chemical shift imaging (CSI) techniques. Diffusion-weighted studies showed a statistically significant inverse correlation with perfusion MRI studies. ADC has been established as having an inverse correlation with the choline MRS signal (11). The Cho signal intensity is indicative of cell proliferation and hence, of the presence of neoplastic tissue. It can be utilized to measure the proliferative potential when spatial indices of tumor growth and angiogenesis are available. To the best of our knowledge, there have been no reports of the use of MRSI examining angiogenesis and its spatial variation in the context of human brain tumors.

MRSI has been used with automated segmentation for better delineation of tumors (12). MRS techniques have also been applied to ex vivo tissue samples, yielding significant information that aids in distinguishing active tumor tissue from healthy tissue, edema, and/or radiation necrosis (13). From a patho-physiological perspective, tumor cel-

lularity and vascularity may be related, which makes any correlates between hemodynamics and biochemistry a critical component of understanding tumor metabolism.

Several significant metabolite correlations have been proposed which suggest that crucial aspects of tumor proliferation like neuronal damage, energy metabolism, hypoxia, necrotic transformation, and metastases may be better understood by using techniques that provide biochemical information. Tumor heterogeneity has also been analyzed using spectroscopic techniques (14). Ratios of metabolites, especially Cho/NAA and lactate/lipid, were useful in distinguishing high-grade tumors from low-grade ones. In a recent metabolite study (15), the ratios of NAA/Cre, NAA/Cho, Cre/Cho, NAA/H_2O, and Cre/H_2O were significantly decreased in high-grade gliomas compared to those in normal brain. The NAA/H_2O and NAA/Cho ratios were significantly reduced in high-grade gliomas in comparison with low-grade gliomas. Spectroscopically, the difference between anaplastic astrocytoma (AA) and GBM is often the presence, or absence, of necrosis.

In a large study characterizing brain tumor metabolism (16), it was found that higher grade tumors had a prominent lipid signal. The lipid signal correlates with cellular necrosis, and it has been hypothesized that these lipid signals originate from mobile fatty acids at the end stage of metabolic insult that precedes cell death. Lipids and lactate correlate with necrosis in high-grade gliomas and may be used in determining tumor grade, although their presence is not specific to high grade tumors. This is significant because studies (17) have reported that relative CBV did not successfully discriminate between AA and GBM. Hemodynamic studies of tumors that offer insight into the angiogenesis potential (4) can be combined with analyses of their biochemistry to characterize tumor vascularization and the resultant disease progression.

MATERIALS AND METHODS

MR Spectroscopy and Imaging

All MRI and spectroscopy were performed on a clinical 3T scanner (Intera, Philips Medical Systems, The Netherlands). Two newly diagnosed brain tumor patients were imaged before any therapeutic and/or surgical intervention (baseline). These patients will be followed up every eight weeks hereafter to obtain longitudinal perfusion and spectroscopic imaging data. The protocol to image these patients is currently active and patient recruitment is ongoing. The patients provided informed consent, approved by the University of Alabama at Birmingham Institutional Review Board and hospital committees overseeing human experiments.

The MRI protocol consisted of T1-weighted (TR/TE = 400 msec/12 msec) scout images followed by axial fluid-attenuated inversion recovery (FLAIR) images. These acquisitions were followed by the 2D chemical shift imaging (2D-CSI) sequence, run on an axial slice from the scout series. After automated shim optimization, the CSI spatial localization box inside the fat suppression slabs was positioned so as to cover the tumor region and include contralateral normal tissue, to provide a reference for postprocessing and analyses. The TR was 1500 msec and the TE was 80 msec for the CSI acquisition. During measurement, water suppression was achieved by applying a chemical shift selective saturation (CHESS) pulse (18). Total acquisition time for the CSI sequence was around 12 minutes, with an additional 3 minutes for shim-optimizing before spectroscopic acquisition.

CSI was followed by the DSC-MRI sequence for perfusion studies. The gradient spin echo (GRASE) (19) with TR/TE of 1900/65 msec, and a 128 x 128 matrix, a field of view (FOV) of 25 cm x 25 cm was used. Thirty 3.5 mm slices were imaged. The total

DSC-MRI scan time was less than 2 minutes. All slices were parallel to the CSI acquisition slice, to allow correlation of perfusion and spectroscopic imaging data at the CSI slice. We used Magnevist (Gadopentate dimeglumine, Berlex Laboratories, Seattle, WA), a gadolinium based contrast agent, injected at a concentration of 0.2 mmol/kg of patient body weight. The contrast agent was injected with a power injector at a flow rate of 4.0 ml/sec and an injection delay of 10 seconds. Spin echo post-contrast T1-weighted images (TR/TE of 450/10 msec) were acquired after perfusion imaging, for anatomic reference.

Analysis of MRSI Data

The spectroscopic imaging data were exported to the XUNspec 1 analysis package (Philips Medical Systems, Best, The Netherlands), running on a Sun Blade 100 (Sun Microsystems, Santa Clara, CA), for offline processing. The raw 2D-CSI data were Fourier transformed in the k_x and k_y directions first. The data were zero-filled to 2048 points to improve the spectral resolution. Gaussian apodization and direct current (DC) offset correction were performed. Time domain filtering was applied to eliminate the residual water peak using the Lanczos HSVD filter (20, 21). The data were then Fourier transformed again to yield a stack of spectra, one per voxel. Levels of Cho, Cre, NAA, and Lac/Lipid were estimated as the peaks at 3.2, 3.0, 2.0, and 1.0 – 1.5 parts per million (ppm), respectively, and used to generate 24 x 24 metabolite maps. No peak quantitation was performed.

Analysis of Perfusion Data

Postprocessing and perfusion analysis were performed using the MedX software (version 3.4.2, Medical Numerics, Sterling, VA) running on a Sun Blade 1000 work-

station. The data sets were prepared for postprocessing by inspection for quality, masking, and generation of parametric maps. Masking of the functional data was performed to ensure accurate determination of arterial input function and to avoid curve-fitting of pixels outside the brain.

A two-stage automatic algorithm (22) was used for identifying arterial voxels in the DSC-MRI data and constructing the arterial input function (AIF). The relative CBV maps were determined though gamma variate fitting (23) of the concentration curves and integration. The relative CBF maps were generated from the amplitude of the residue curve that results from deconvolution of the tissue curve via singular value decomposition.

The angiogenesis potential ($\mathcal{A}$) maps were generated using the CBF, CBV, and T2* recovery information, computed from the T2* susceptibility perfusion data sets (4). A value of k = 1 was used for computation of the $\mathcal{A}$ maps.

Correlation of Perfusion and Spectroscopic Imaging

All image analyses and correlative studies were performed using programs custom-written in MATLAB (The Mathworks Inc., Natick, MA). These data were correlated with metabolite images obtained from the 2D-CSI acquisition. Nearest neighbor interpolation was used to reconcile image sizes, because perfusion images (128 x 128), post-contrast T1 weighted images (512 x 512) and metabolite maps (24 x 24) had different matrix sizes.

RESULTS

Figures 1 and 2 show anatomic images, CBF maps, and spectroscopic images, from patient 1 and 2, respectively. Figures 3 and 4 show the spectra from voxels in patient 1 and patient 2, respectively. We illustrate the differences in metabolite peaks in three distinct regions of the patients: healthy brain tissue, tumor fringes, and tumor core. Spectra from these three regions are shown in green, blue, and red, respectively.

In our experience (5), CBF has been reliable as a quantitative surrogate of angiogenesis in human brain tumor drug trials. We present only the CBF maps in this report, although CBV values have been tabulated in subsequent sections of this paper.

Both patients showed similar spectra obtained from healthy tissue, with well-resolved Cho and NAA peaks. Patient 2 showed a distinct doublet peak around 1.3 ppm. This is from the lactate/lipid molecules in the voxel that was placed in the tumor fringe area. Both patients also showed a decrease in Cho and a sharp decrease in NAA at the center of the tumor, presumably from necrosis. In the margins of the tumors, the levels of Cho were elevated and the NAA peak was lower. Patient 2 also showed a decrease in the Cre peak, at 3.0 ppm in the tumor fringes.

Figure 3c and 4c show profiles of relative CBF, Cho, NAA and Cho/NAA ratio, obtained from a line spanning the FOV, shown in yellow in the respective anatomic images, Figs. 3a and 4a. Both patients showed very low CBF levels at the center of the tumor. Patient 1 showed a distinct increase in relative CBF levels in margins, on both sides of the tumor. In the tumor fringe areas, where CBF was significantly elevated, both patients showed increased Cho levels and decreased NAA. We noticed considerable variations in the Cho and NAA peaks in areas surrounding the tumor core. Creatine in the tumor fringes was higher in patient 1, and lower in patient 2. Cho and NAA were consis-

tently lower in the tumor core for both patients. Also, as shown in Fig 2b, patient 2 had low relative CBF levels overall.

The relative CBF and CBV values from the color-coded ROIs in Figs. 3 and 4 are shown in Tables 1 and 2, respectively. These were computed with respect to the mean value of these parameters in healthy tissue, using 25 pixel ROIs, in the contralateral hemisphere of the patient.

Table 1
Relative CBV and CBF Values for Patient 1

ROI	Relative CBF (Mean for 25 pixel ROI)	Relative CBV (Mean for 25 pixel ROI)
Healthy tissue	1.01	1.03
Tumor fringe area	3.56	3.13
Tumor core	0.26	0.29

Table 2
Relative CBV and CBF Values for Patient 2

ROI	Relative CBF (Mean for 25 pixel ROI)	Relative CBV (Mean for 25 pixel ROI)
Healthy tissue	1.00	1.03
Tumor fringe area	2.82	2.65
Tumor core	0.13	0.17

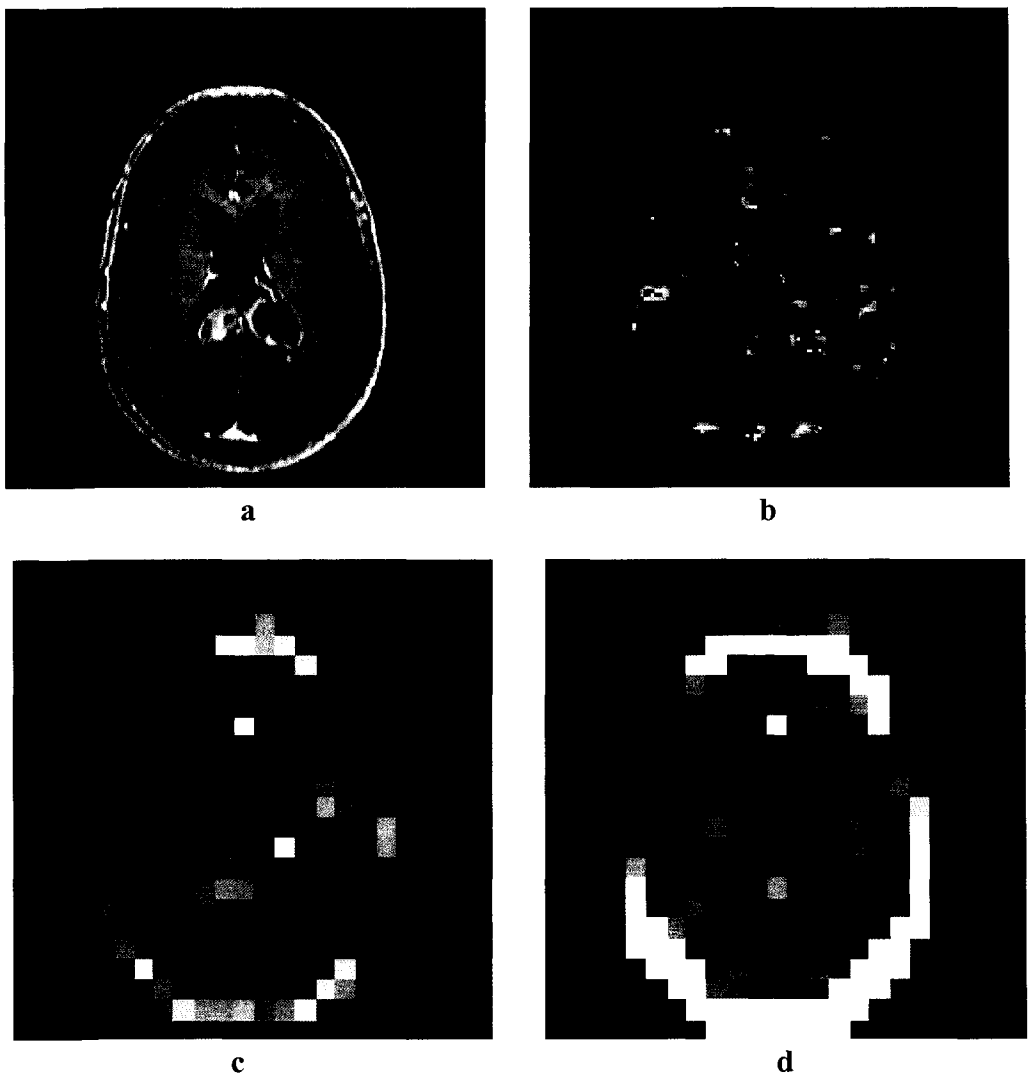

Figure 1. Patient 1: Comparison of hemodynamic and spectral data. **a:** Post-contrast T_1 weighted image. **b:** Corresponding relative CBF map. **c:** Cho image. **d:** NAA image.

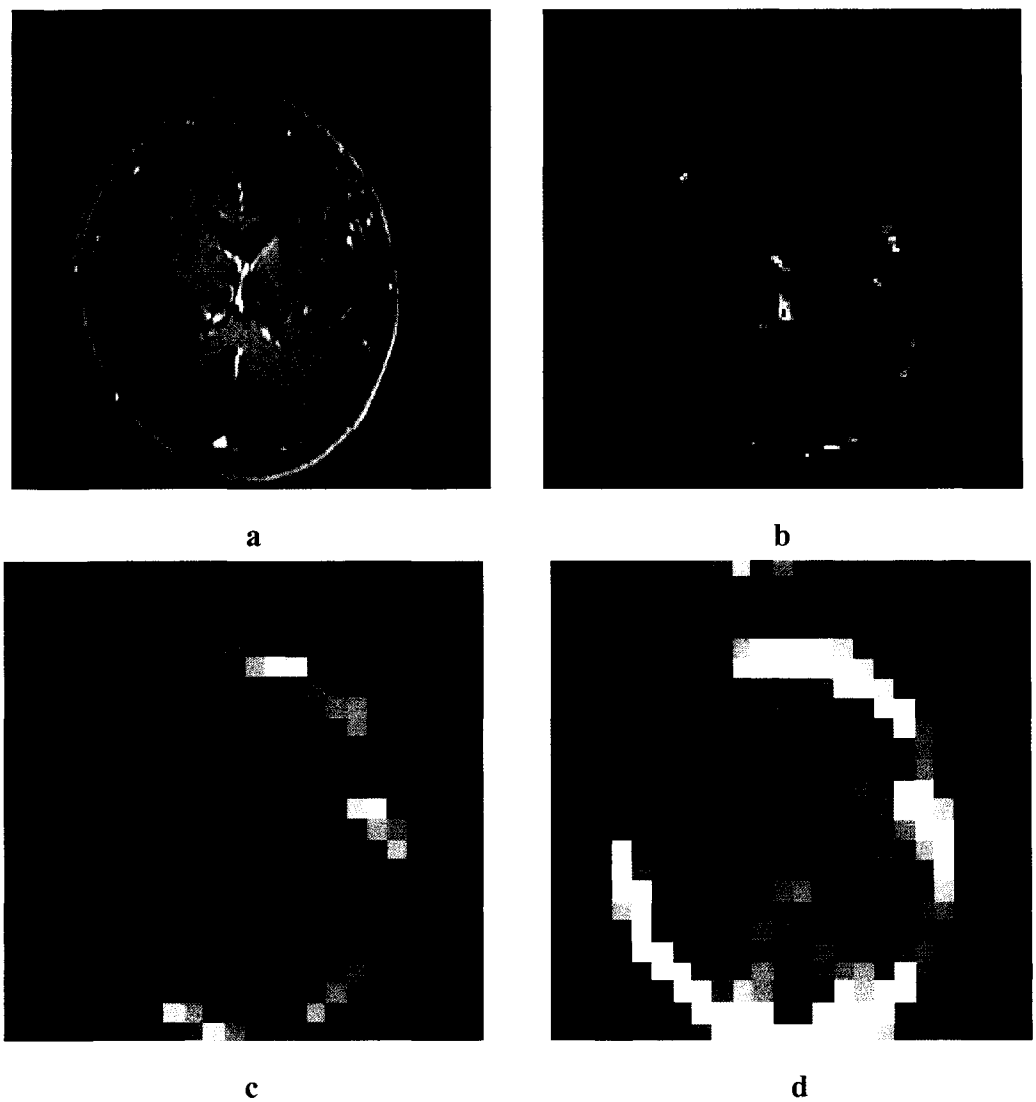

Figure 2. Patient 2: Comparison of hemodynamic and spectral data. **a:** Post-contrast T_1 weighted image. **b:** Corresponding relative CBF map. **c:** Cho image. **d:** NAA image.

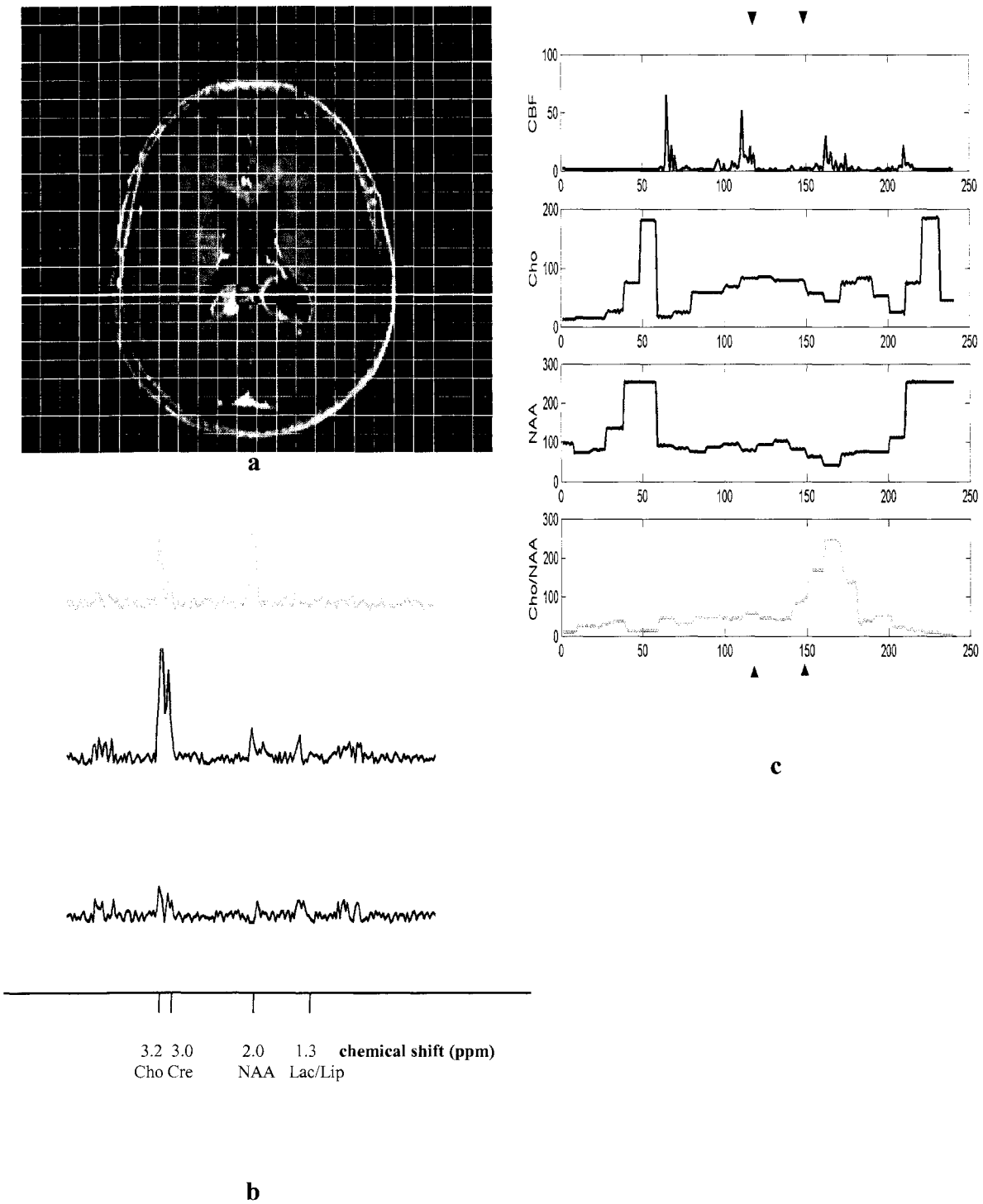

Figure 3. Patient 1: Correlation of spectroscopic and hemodynamic data. **a:** Anatomic Image showing the 24 x 24 spectral grid. **b:** Individual spectra from voxels in healthy tissue (green), tumor margin (blue), and tumor core (red). **c:** relative CBF, Cho, NAA and Cho/NAA ratio profiles from the yellow line in 3a. The black triangles indicate tumor margins.

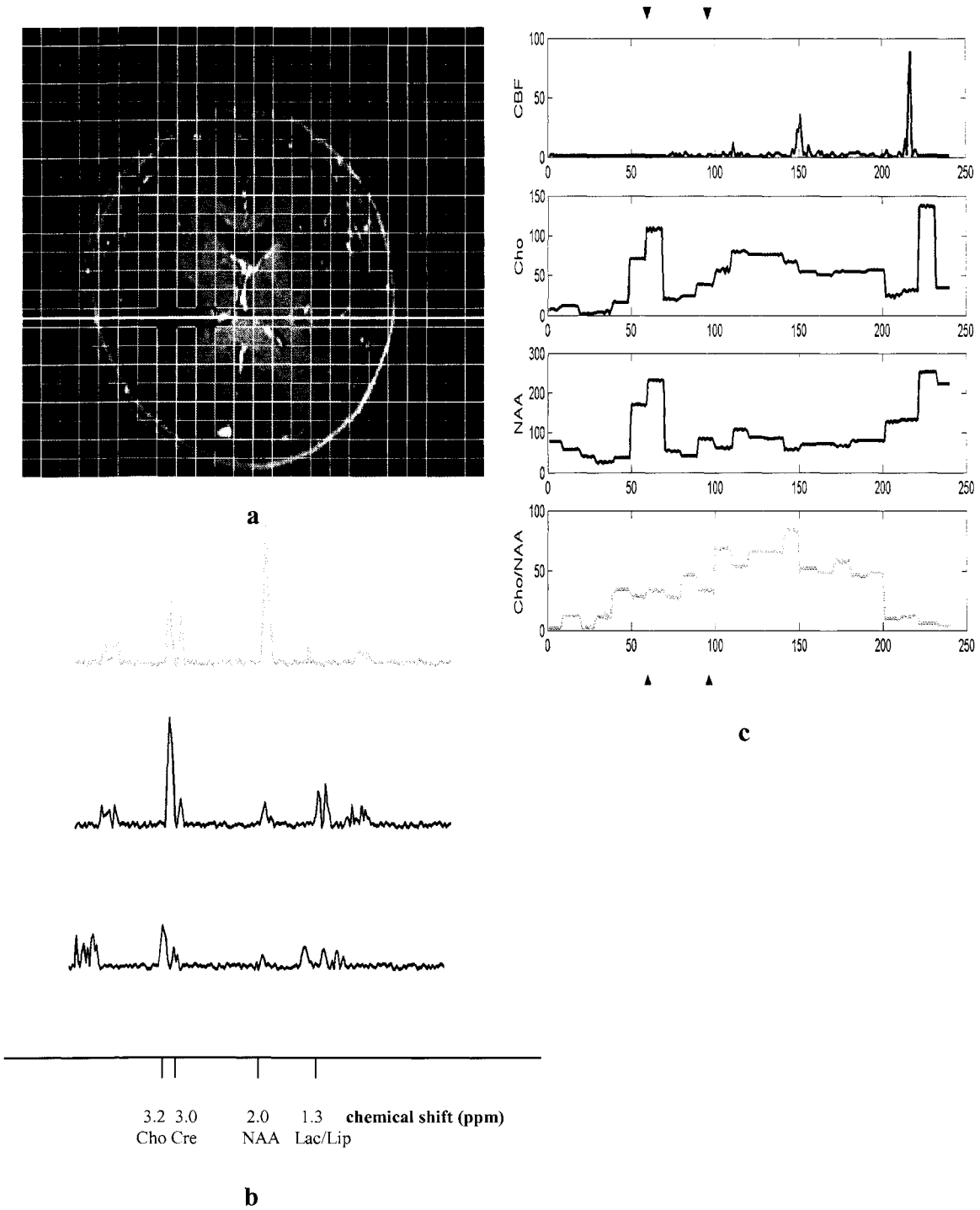

Figure 4. Patient 2: Correlation of spectroscopic and hemodynamic data. **a:** Anatomic Image showing the 24 x 24 spectral grid. **b:** Individual spectra from voxels in healthy tissue (green), tumor margin (blue), and tumor core (red). **c:** relative CBF, Cho, NAA and Cho/NAA ratio profiles from the yellow line in 4a. The black triangles indicate tumor margins.

The angiogenesis potential maps for both patients are presented in Fig. 5 along with the Cho/NAA ratio maps. The $\mathcal{A}$ map for patient 1 (Fig. 5(a)) shows increased angiogenesis potential in the "ring" surrounding the tumor and in a fringe area in the contralateral hemisphere. Patient 2 did not show significant angiogenesis, as estimated by our technique.

The Cho/NAA ratio images demonstrate hotspots, at areas that correspond to the tumor, seen in both patients in Figs 5c and 5d, respectively. Patient 2 did not demonstrate significant enhancement, and though the hemodynamics did not suggest a high-grade tumor, the metabolite distribution is suggestive of a malignant neoplasm. The spatial locations of areas high in the Cho/NAA maps confirm that the angiogenesis potential maps are fairly accurate in discerning areas that might be angiogenic and illustrate the utility of spectral information when used alongside quantitative hemodynamic information.

DISCUSSION

Although blood flow and volume in brain tumors have been analyzed by several groups along with metabolite distributions measured using MRSI techniques, there have been relatively few papers describing their utility in evaluating angiogenesis, a critical process in tumor growth and invasion. In this work, we report correlations between Cho, NAA, and $\mathcal{A}$, the angiogenic potential, and demonstrate that concentrations of metabolites indeed match the spatial variation of estimates of angio-architecture in brain tumors. Values of the Cho/NAA ratios were high in tumor regions, in agreement with similar observations published earlier (7). The Cho/NAA ratio correlates with tumor location but not does necessarily correlate with areas of high $\mathcal{A}$. This ratio is traditionally preferred over others like Cho/Cre for two reasons:

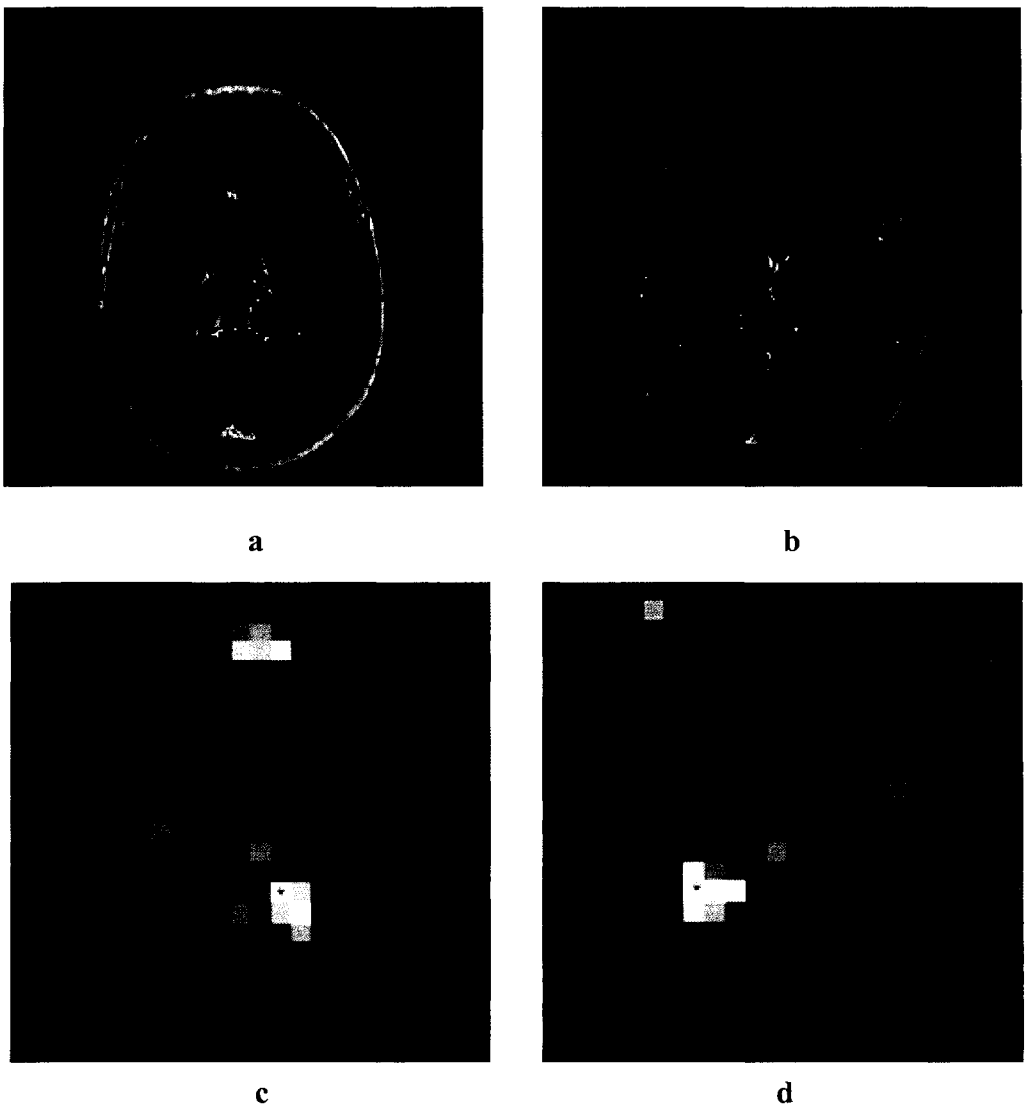

Figure 5. Angiogenesis potential and Cho/NAA ratio maps. **a:** Angiogenesis potential map for patient 1. **b:** Angiogenesis potential map for patient 2. **c:** Cho/NAA ratio image for patient 1. **d:** Cho/NAA ratio image for patient 2. The red asterisks indicate the tumor centroid in each image, placed to enable comparison of $\mathcal{A}$ maps with Cho/NAA ratios.

1. The signal-to-noise ratio (SNR) of the NAA signal is much higher than Cre or any other metabolite, and
2. The variability of Cre in brain tumor pathology is far greater than that of NAA.

2D-CSI was chosen as the acquisition sequence for spectroscopic imaging because it combines the features of both imaging and spectroscopy (24). It is also well suited to malignant brain cancer studies since single-voxel spectroscopy techniques do not accurately characterize the heterogeneity of high-grade tumors. CSI is a technique for collecting spectroscopic data from multiple adjacent voxels covering a large volume of interest in a single measurement. In 2D-CSI, spatial localization is done by phase encoding in two dimensions. A 2D Fourier transform yields localized spectra. The version of 2D-CSI used in our spectroscopic acquisition was combined with a slice selection excitation in order to produce voxels of approximately 1 cm^3 in about 12 minutes using a standard imaging head coil. This, combined with perfusion and anatomic image acquisitions, resulted in a total imaging time of around 35 minutes for the brain tumor patients. We used standard automated second-order shimming routines available on the scanner. Further improvements in SNR are possible by applying postprocessing software-based methods (25) that correct for eddy current distortions by measuring the distortions of a reference signal.

Since the primary focus of our correlative study was on spatial distributions of metabolites and their comparison with hemodynamic parameters, we did not attempt to perform absolute peak quantitation of the metabolites being imaged. Use of more refined spectroscopic postprocessing algorithms could be considered to obtain such values of concentrations. The utility of spectroscopic imaging data in therapeutic evaluations of

angiogenesis will be greatly enhanced by quantitating metabolites and their distribution in vivo. The comparative studies could also be extended to three spatial dimensions for more comprehensive assessment of tumor angiogenesis and growth. Longitudinal measurements of spectral information could also be used in monitoring of therapy efficacy in brain tumor patients.

Gadolinium-based contrast agents, like Magnevist used in our study, shorten the T1 relaxation time of the metabolites, increasing their signal contributions, especially during short TR scans. Local tissue susceptibility may also be shortened by the contrast agent, reducing T2* and causing line broadening. Some studies suggest that good quality spectra may be obtained from MR spectroscopic studies performed after contrast administration, although there is widespread disagreement on this issue. It has been argued that the effects of contrast administration on levels of metabolites like Cho, Cre, and NAA are minimal because these metabolites are almost entirely intracellular and hence are not exposed to gadolinium. A 15% decrease in Cho levels has been reported following gadolinium-based contrast administration (26). Our data was unaffected by contrast administration because 2D-CSI was performed before contrast administration.

Increased Cho is suggestive of cell proliferation (27) and has been reported in astrocytomas. Choline has also been associated with myelin breakdown and the Cho peak might contain information related to cell density. Both the patients studied in this work had elevated Cho peaks at 3.2 ppm in the tumor fringe areas, shown in Figs. 3b and 4b. These are in agreement with data published by several groups earlier and support the hypothesis that angiogenic and mitotic activity are increased in the tumor fringe areas. An increase in membrane synthesis in proliferating cells and increased membrane turnover contribute to elevated levels of Cho. Though it is agreed that the Cho resonance peak is

generated by the nine protons in the $(CH_3)_3$ group of the Cho molecule, several aspects of the peak composition remain unexplained including the variation of the spectra with abnormal pathology.

The N-acetyl aspartate peak at 2.0 ppm is another major peak in the normal adult brain and acts as a neuronal and axonal marker. It drops sharply in areas that are hypoxic and necrotic. In both our patients, there were significant decreases in the NAA peaks, observed both in tumor fringe areas, and in the tumor cores. Residual peaks around the 2.0 ppm mark are either from contamination due to tumor infiltration into normal tissue and/or from the partial volume effect. The elevated NAA peaks seen in spatial profiles of both patients are likely due to contamination by fat from nearby tissue, seen as bright areas in Figs. 1d and 2d. This could be eliminated by more efficient lipid suppression routines before the CSI acquisition. Both NAA and Cho concentrations are in agreement with earlier reports of biochemical profiles of necrotic and proliferative areas.

MRS does suffer from poor sensitivity in the context of assessment of tumor vasculature (28). Spectroscopy has been used in animal models to assess effects of blood flow modifiers such as nicotinamide and carbogen (29). Advances in spectral data processing and increase in spatial resolution will be required to make metabolite maps and spectral data a reliable component of the clinical analyses of angiogenesis.

We have shown that tumor characteristics obtained from quantification of hemodynamics and those extracted from MRSI techniques are in agreement. Merging the two threads validates a multi-compartment model of brain tumors proposed earlier (30,31). These models did not, however, study angiogenesis and/or the spatial variation of parameters that influence tumor proliferation. Correlating the spatial variation of parameters obtained through perfusion MRI and MRSI modalities provides valuable information

about growth and invasion patterns of gliomas. The addition of a priori information, radiological and/or histological, could improve the characterization of spatial heterogeneity in tumors. It will require analyses of larger patient populations to validate the statistical significance of correlative approaches that incorporate hemodynamics as well as spectroscopic information. Such quantitative approaches would be valuable in measuring cancer aggression, biopsy guidance, and the planning and monitoring of brain tumor therapy.

ACKNOWLEDGMENTS

We thank Dr. William T Evanochko, Billy Fisher, and Cathy Clements in the UAB Cardiovascular MRI section, for their help with MR imaging and spectroscopy. We used the computing facilities of the Center for Nuclear Imaging Research (CNIR) for spectroscopic data processing. This work was supported by NIH grant R21 CA 091560 to L.B.N.

REFERENCES

1. Folkman J. What is the evidence that tumors are angiogenesis dependent? J Natl Cancer Inst 1990;82:4-6.

2. Nelson SJ. Multivoxel magnetic resonance spectroscopy of brain tumors. Mol Cancer Ther 2003;2:497-507.

3. Möller-Hartmann W, Herminghaus S, Krings T, et al. Clinical application of proton magnetic resonance spectroscopy in the diagnosis of intracranial mass lesions. Neuroradiology 2002;44(5):371-381.

4. Akella NS, Twieg DB, Nabors LB. Quantitative estimation of angiogenesis in vivo. In: Proceedings of the 13th Annual Meeting of ISMRM, Miami, 2005.

5. Akella NS, Twieg DB, Mikkelsen T, et al. Assessment of brain tumor angiogenesis inhibitors using perfusion magnetic resonance imaging - quality and analysis results of a phase I trial. J Magn Reson Imaging 2004;20: 913-922.

6. Stubbs M. Application of magnetic resonance techniques for imaging tumor physiology Acta Oncol 1999;38:845-853.

7. Nelson SJ. Analysis of volume MRI and MR spectroscopic imaging data for the evaluation of patients with brain tumors. Magn Reson Med 2001;46:228-239.

8. Howe FA, Barton SJ, Cudlip SA, et al. Metabolic profiles of human brain tumors using quantitative in vivo ^{1}H magnetic resonance spectroscopy. Magn Reson Med 2003;49:223-232.

9. Law M, Yang S, Wang H, et al. Glioma grading: sensitivity, specificity, and predictive values of perfusion MR imaging and proton MR spectroscopic imaging compared with conventional MR imaging. AJNR Am J Neuroradiol 2003;24:1989-1998.

10. Yang D, Korogi Y, Sugahara T, et al. Cerebral gliomas: prospective comparison of multivoxel 2D chemical-shift imaging proton MR spectroscopy, echoplanar perfusion and diffusion-weighted MRI. Neuroradiology 2002;44:656-666.

11. Gupta RK, Sinha U, Cloughesy TF, Alger JR. Inverse correlation between choline magnetic resonance spectroscopy signal intensity and the apparent diffusion coefficient in human glioma. Magn Reson Med 1999;41:2-7.

12. Stadlbauer A, Moser E, Gruber S, et al. Improved delineation of brain tumors: an automated method for segmentation based on pathological changes of 1H-MRSI metabolite in gliomas. Neuroimage 2004;23:454-461.

13. Peeling J, Sutherland G. High resolution ^{1}H NMR spectroscopy studies of extracts of human cerebral neoplasms. Magn Reson Med 1992;24:123-136.

14. Li X, Lu Y, Pirzkall A, McKnight T, Nelson SJ. Analysis of the spatial characteristics of metabolic abnormalities in newly diagnosed glioma patients. J Magn Reson Imaging 2002;16:229-237.

15. Tong Z, Yamaki T, Harada K, Houkin K. In vivo quantification of the metabolites in normal brain and brain tumors by proton MR spectroscopy using water as an internal standard. Magn Reson Imaging 2004;22:735-742.

16. Negendank W, Sauter R. Intratumoral lipids in 1H MRS in vivo in brain tumors: experience of the Siemens cooperative clinical trial. Anticancer Res 1996;16:1533-1538.

17. Knopp EA, Cha S, Johnson G, et al. Glial neoplasms: dynamic contrast enhanced T2* -weighted MR imaging. Radiology 1999;211:791-798.

18. Haase A, Frahm J, Hanicke W, Matthaei D. 1H NMR chemical shift selective (CHESS) imaging. Phys Med Biol 1985;30:341-344.

19. Oshio K, Feinberg DA. GRASE (Gradient- and Spin-Echo) imaging: A novel fast MRI technique. Magn. Med. Med 1991;10:344-349

20. Pijnappel WWF, van den Boogaart A, de Beer R, van Ormondt D. SVD-based quantification of magnetic resonance signals. J Magn Reson 1992;97:122-134.

21. van den Boogaart A, van Ormondt D, Pijnappel WWF, de Beer R, Ala-Korpela M. Removal of the water resonance from ^{1}H magnetic resonance spectra. In: McWhirter JG, ed. Mathematics in Signal Processing III. Oxford, England: Clarendon Press; 1994:175-195.

22. Morris ED, Tasciyan TA, VanMeter JW, Maisog JM, Zeffiro TA. Automated determination of the arterial input function for MR perfusion analysis. In: Proceedings of the 8th Annual Meeting of the ISMRM, Denver, 2000.

23. Ostergaard L, Weisskoff RM, Chesler DA, Gyldensted C, Rosen BR. High resolution measurement of cerebral blood flow using intravascular tracer bolus passages. Part I: mathematical approach and statistical analysis. Magn Reson Med 1996;36:715-725.

24. Salibi N, Brown MA. Clinical MR Spectroscopy: First Principles. New York: John Wiley and Sons; 1998. 220 p.

25. Klose U. In vivo proton spectroscopy in presence of eddy currents. Magn Reson Med 1990;14:26-30.

26. Sijens PE, van den Bent MJ, Nowak PJ, van Dijk P, Oudkerk M. 1H chemical shift imaging reveals loss of brain tumor choline signal after administration of Gd-contrast. Magn Reson Med 1997; 37:222-225.

27. Kugel H, Heindel HW, Ernestus R-I, Bunke J, du Mesnil R, Friedmann G. Human brain tumors: spectral patterns detected with localized H-1 MR spectroscopy. Radiology 1992;183:701-709.

28. Anderson H, Price P, Blomley M, Leach MO, Workman P. Measuring changes in human tumor vasculature in response to therapy using functional imaging. Br J Cancer 2001; 85:1085-1093.

29. Robinson SP, Howe FA, Stubbs M, Griffiths JR. Effects of nicotinamide and carbogen on tumor oxygenation, blood flow, energetics, and blood glucose levels. Br J Cancer 2000;82:2007-2014.

30. Ott D, Hennig J, Ernst T. Human brain tumors: assessment with in vivo proton MR spectroscopy. Radiology 1993;186:745-752.

31. Tzika AA, Vajapeyam S, Barnes P. Multivoxel proton MR spectroscopy and hemodynamic MR imaging of childhood brain tumors: preliminary observations. AJNR Am J Neuroradiol 1997;18:203-218.

CONCLUSIONS

MRI and MRS are powerful tools to study the invasion and proliferation of brain cancer, resultant changes to hemodynamic characteristics, and the impact on variations in cerebral biochemistry. In this dissertation, the broad goals were to establish the feasibility of using relative cerebral blood flow and volume as a marker of brain tumor angiogenesis and devise a framework where CBV and CBF could be measured and tracked longitudinally in patients with primary brain cancer. A technique was also developed to quantitate angiogenesis in vivo. Finally, spectroscopic imaging was used to obtain metabolite distributions and study spatial variation of tumor signatures alongside their hemodynamics.

We have demonstrated that CBF and CBV could be used as surrogates of tumor angiogenesis in a large multi-institution study involving over thirty patients. Considerable time was spent in acquiring MR data that were subject to stringent quality tests and developing the analyses methodology to enable both inter- and intra-patient assessment. Statistical thresholds for goodness of the gamma variate fit, T2* recovery, and mean signal full-width at half-minimum were computed for our data sets with a 99% one-sided confidence interval. Several of these patients were monitored for longitudinal changes in hemodynamics, and quality thresholds were calculated for perfusion data sets. The results of analysis of CBV and CBF were correlated with clinical responses of the patients studied and it was shown, with statistical significance, that a systematic study of the aforementioned indices could provide reliable measures of tumor angiogenesis in vivo. It was

established that malignant brain tumors have altered perfusion parameters, as assessed by DSC-MRI, which may be used to understand and monitor neovascularization.

While standard radiological investigations can provide information regarding the spatial location of brain tumors, treatment is usually decided by results of invasive biopsies. In malignant tumors, the blood brain barrier has been thought of as a critical factor in determining the grade, in part because of the relationship between permeability and angiogenesis. Permeability could be due to increased levels of vascular endothelial factor (VEGF), a factor that is responsible for the growth of blood vessels. Perfusion maps and sophisticated postprocessing techniques could provide valuable information concerning blood flow, volume, and the blood brain barrier permeability, which would make tumor characterization more reliable.

A common feature of malignant gliomas is the disruption of the blood-brain barrier resulting in the extravasation (17) of gadolinium-based contrast agents into the interstitial space. Glial cells typically infiltrate into brain parenchyma as a result of neoplasms, usually along paths of least resistance. The biomechanical consequences of these cell-shifts could disrupt vessel integrity. Typically, the capillaries are disrupted making the vessels in the tumor-affected area more permeable or "leaky." The resulting misestimation of blood flow and volume obtained through methods like DSC-MRI has been studied by several groups, and this is of special interest to quantitative analyses of hemodynamics such as ours. Several correction strategies have been published that account for both the T1 and T2* effects. The use of large particles like MIONS, endogenous contrast agents, and arterial spin labeling (ASL) techniques, which bypass such effects, are being tried in various animal and human models investigating tumor vasculature. Advanced

molecular imaging techniques that "tag" certain physiology-specific processes are also becoming popular among groups investigating cancer.

As it becomes apparent that understanding tumor vascularization could hold the key to unraveling the phenotype of several cancers, the focus moves from identifying non-invasive imaging-based markers to the search for reliable quantitative measures that enable predictive and diagnostic assessment. There are several groups, including ours, currently investigating animal models of human brain cancer using magnetic resonance and other imaging modalities. The role of angiogenesis in the sustenance and proliferation of cancer, especially brain cancer, is being appreciated at several levels: imaging, pharmaco-kinetic, molecular, and genetic. As evidenced by the growing number of anti-angiogenic cancer therapies (7), the quantitative study of angiogenesis guided by in vivo MRI correlates has the potential to be a valuable tool in the clinical assessment of malignant brain tumors and offers several therapy-planning options for neuro-oncologists.

Brain tumors are histologically very heterogeneous, a fact not always obvious in non-invasive anatomic and functional imaging techniques such as DSC-MRI. A large part of our emphasis in mapping angiogenesis was quantitating the underlying spatial variation. Considerable efforts will be required to develop reliable image co-registration algorithms which enable multi-modality comparisons of structural and functional aspects of tumor pathology. Appropriate verification of quantitative estimates will have to be made using brain tumor histology and other techniques, some of which are invasive. Given the inherent heterogeneity of most malignant gliomas, the extension of models such as the one proposed in this work, to three spatial dimensions, will be required for more accurate evaluation of brain tumors. It has also been speculated (18) that tumor vessels are highly

permeable and extravasate fluid, hence increasing the local tissue pressure around tumor vessels. The balance between decreased intravascular pressure and increased interstitial fluid pressure may result in dynamic alterations of blood flow in tumor micro-vessels. This often leads to intraluminal platelet deposition and thrombosis, leading to focal areas of necrosis and tumor-associated hemorrhage. These changes may be identified by a combination of MRI feature changes and incorporated into hemodynamic changes associated with malignant tumors. These could lead to a better understanding of the angiogenesis cascade (19) and the associated variations in angio-architecture and biochemical modulations.

A very useful application of our technique is the longitudinal tracking of therapy in patients with brain tumors. As evidenced by the studies on patient 2 (preprint 2), it is possible to apply the method to series perfusion studies in an attempt to evaluate the temporal changes in tumor hemodynamics. This patient demonstrated no clinical response to cilengitide therapy. While increased tumor enhancement due to growth was seen in the post-contrast T1 images, quantification of angiogenesis on a pixel-by-pixel basis provided additional information about the vasculature and hemodynamics. In addition to increases in CBV, CBF, and $\mathcal{A}$, patient 2 demonstrated an outward shift of about 18 pixels in the $\mathcal{A}$ peak. The evolution of tumor hemodynamics over time could very well be a reliable tool in evaluating disease progression. Co-registration of intra-patient data sets is of little consequence since the parameters being analyzed are reported with respect to a tumor centroid, computed individually for each study.

More recently, "normalization" of anti-angiogenic therapy has been proposed as a more effective strategy in combating cancer (20). This will require frequent and efficient

in vivo monitoring of the delicate balance between glioma vascularization, therapeutic interventions, and drug uptake, as well as physiological conditions like stress, hypoxia, and the tumor micro-environment. Strengthening the imaging-based evaluations of tumors in vivo will allow us to monitor these aspects non-invasively.

Limitations of MRI/S techniques include decreased sensitivity to calcification and lack of specificity; several pathologies have similar presentations (e.g. infarcts, demyelnation, abscesses). Enhancement on DSC-MRI does not equate to tumor grade and also does not delineate borders of tumor cells. Techniques like the one proposed in the second manuscript that quantify angiogenesis will need to be developed and perfected to understand the spatial complexity of malignant tumors.

In addition to the study of hemodynamics, we have imaged and analyzed metabolite distributions in brain tumor patients. Up to this point, much of the metabolic imaging has been done using either magnetic resonance spectroscopy or nuclear medicine technologies such as positron emission tomography (PET) and single-photon emission computed-tomography (SPECT). PET studies of tumor metabolism using 18-fluoro-deoxyglucose have been used in distinguishing metabolically active areas from necrotic regions. These studies have shown that glucose utilization is a predictor of prognosis in brain lesions (21). For the most part, MRS techniques have relied on single-voxel techniques because comprehensive examinations could easily take over one hour for obtaining biochemical information alone. With several technological and computational hurdles now cleared, faster, more efficient spectroscopic imaging techniques are being tested and implemented on commercially available clinical MR scanners. Significant improvements in the signal-to-noise ratio and spatial resolution are also critical to making spectroscopy

a clinically viable investigational tool for brain tumors. Spectroscopic imaging greatly enhances the diagnostic utility of conventional functional and anatomic MR imaging. Our data demonstrate that brain tumor pathology is well suited to interrogation by spectroscopic imaging techniques.

The Cho/NAA ratio images from the patients examined showed good spatial correlation with areas of altered hemodynamics, corroborating that the angiogenesis potential estimated by our technique indeed identifies areas of abnormal pathology. This illustrates the utility of spectral information when used alongside quantitative hemodynamic information. MR spectroscopy techniques have shown promise in distinguishing necrosis from recurrent tumors (22), a fact that makes them attractive to characterizing angiogenic areas surrounding malignant tumors.

Another analysis tool that is used in interpreting MR spectra is absolute quantitation of peaks. Since establishing a framework to compare hemodynamics and biochemical distributions was our chief objective, we have not attempted peak quantitation. Routinely used gadolinium-based contrast agents shorten the relaxation times of the metabolites being imaged. While some studies suggest that reasonably good quality spectra may be obtained after contrast administration, there is no clear consensus on how administration of contrast agents affect spectral peaks. Consequently, all spectroscopic image acquisitions were performed before administration of contrast.

Future directions for the continuation of the research presented in this dissertation would include addition of statistical significance to the results presented herein, especially the MRSI and correlations between hemodynamics and biochemistry. The role of white matter tracts in the invasion of cancer is of special interest in brain tumor pathol-

ogy. The addition of modalities that quantitatively map the role of tracts such as diffusion tensor imaging would strengthen mathematical modeling approaches aimed at understanding the angiogenic cascade. It is also recommended that MR imaging and spectroscopy be coupled with histological measurements that further validate multi-compartment models in tissue classification, especially in studies involving animal models.

Inclusion of a priori information such as tumor shape attributes and more sophisticated geometric modeling might enhance the accuracy of estimates of angiogenesis. For example, the annular model used to compute the angiogenesis potential could be replaced with a tumor-shaped region. Extension of the modeling approaches to three spatial dimensions would also make the estimates more realistic. The addition of physiology-specific bio-molecular markers that target processes in the angiogenesis cascade will aid imaging based predictions of angiogenesis.

In conclusion, results, both hemodynamic and spectroscopic, are in agreement with histological characteristics of malignant brain tumors (2). The data acquired and analyzed suggest that a three- or possibly four-compartment model is ideally suited for analysis of progression of brain cancer. Based on CBF, CBV, $\mathcal{A}$, and distribution of metabolites like Cho and NAA, it is suggested that characterization of tissue in vivo be performed as healthy tissue, angiogenic region, necrosis and a fourth region, that includes metastases, areas of abnormal mitosis, vasogenic edema, and other effects of neoplastic activity. The systematic study of the "angiotype" of a tumor, reflecting the behavior of the blood vessels nourishing it, and the capillary network patterning (23) that occurs as a result of neovascularization will augment our current understanding of the role of angiogenesis in cancer. Imaging and spectroscopy provide reliable and accurate measures of

angiogenesis that add to the prognostic value of routine radiological and histological examinations.

GENERAL LIST OF REFERENCES

1. Folkman J. Tumor angiogenesis: therapeutic implications. N Engl J Med 1971;285:1182-1186.

2. Burger PC, Scheithauer BW. Tumors of the central nervous system. Washington, D. C.: Armed Forces Institute of Pathology; 1994. 452 p.

3. Folkman J. What is the evidence that tumors are angiogenesis dependent? J Natl Cancer Inst 1990;82:4-6.

4. Hanahan D, Folkman J. Patterns and emerging mechanisms of the angiogenesis switch during tumorigenesis. Cell 1996;86:353-364.

5. Rak J, Croix BS, Krebel R. Consequences of angiogenesis for tumor progression, metastasis, and cancer therapy. Anticancer Drugs 1995;6:3-18.

6. Brem S, Cotran R, Folkman J. Tumor angiogenesis: a quantitative method for histological grading. J Natl Cancer Inst 1972;48:347-356.

7. Goldbrunner RH, Wagner S, Roosen K, Tonn JC. Models for assessment of angiogenesis in gliomas. J Neurooncol 2000;50:53-62.

8. Berger MS and Wilson CB. The Gliomas. Philadelphia, PA: W. B. Saunders company, 1999. p. 87-106.

9. Sorenson AG, Reimer P. Cerebral MR perfusion imaging: principles and current applications. Stuttgart: Georg Thieme Varlag; 2000. 152 p.

10. Rempp KA, Brix G, Wenz FRBC, Guckel F, Lorenz WJ. Quantification of regional cerebral blood flow and volume with dynamic susceptibility contrast-enhanced MR imaging. Radiology 1994;193:637-641.

11. Rosen BR, Belliveau JW, Buchbinder BR. Contrast agents and cerebral hemodynamics. Magn Reson Med 1991;19:285-292.

12. Nelson SJ. Multivoxel magnetic resonance spectroscopy of brain tumors. Mol Cancer Ther 2003;2:497-507.

13. Salibi N, Brown MA. Clinical MR Spectroscopy: First Principles. New York: John Wiley and Sons; 1998. 220 p.

14. Anderson H, Price P, Blomley M, Leach MO, Workman. Measuring changes in human tumor vasculature in response to therapy using functional imaging techniques. Br J Cancer 2001; 85:1085-1093.

15. Akella NS, Twieg DB, Mikkelsen T, et al. Assessment of brain tumor angiogenesis inhibitors using perfusion magnetic resonance imaging - quality and analysis Results of a phase I trial. J Magn Reson Imaging 2004;20: 913-922.

16. Akella NS, Twieg DB, Nabors LB. Quantitative estimation of angiogenesis *in vivo*. In: Proceedings of the 13th Annual Meeting of ISMRM, Miami, 2005.

17. Essig M, Wenz F, Scholdei R, et al. Dynamic susceptibility contrast-enhanced echo-planar imaging of cerebral gliomas, effect of contrast medium extravasation. Acta Radiol 2002;43:354-359.

18. Jain RK. Vascular and interstitial barriers to delivery of therapeutic agents in tumors. Cancer Metastasis Rev 1990;9:253-266.

19. Del Maestro RF, Megyesi JF, Farrell CL. Mechanisms of tumor-associated edema: a review. Can J Neurol Sci 1990;17:177-183.

20. Jain RK. Normalization of tumor vasculature: an emerging concept in antiangiogenic therapy. Science 2005;307:58-62.

21. Alavi J, Alavi A, Charoluk J. et al. Positron emission tomography in patients with glioma: a predictor of prognosis. Cancer 1988;62:1074-1078.

22. Ott D, Hennig J, Ernst T. Human brain tumors: assessment with in vivo proton MR spectroscopy. Radiology 1993;186:745-752.

23. Hansen-Smith FM. Capillary network patterning during angiogenesis. Clin Exp Pharmacol Physiol 2000;27:830-835.

APPENDIX

UAB IRB APPROVAL CERTIFICATION FOR RESEARCH

THE UNIVERSITY OF ALABAMA AT BIRMINGHAM
Institutional Review Board for Human Use

MEMORANDUM

TO: Narasimha Akella

FROM: Ferdinand Urthaler, M.D.
Chairman, IRB

Sheila Moore, CIP
Director, IRB

RE: "Assessment of Brain Tumor Angiogenesis Using Perfusion Magnetic Resonance Imaging and Magnetic Resonance Spectroscopy" – Graduate Thesis

Date: March 24, 2005

As requested, this memorandum should serve as notification that the UAB IRB is in receipt of and has reviewed your expedited application regarding the above-mentioned research project. The OIRB understands that all work involved in the project was conducted without approval from the UAB IRB.

As a UAB student, all research involving human subjects must be submitted to the UAB IRB Office for approval. It appears that you and your mentor, Burt Nabors, were under the impression that since the secondary data analysis for your project was performed using only data from Dr. Nabors' IRB approved clinical trial then no further IRB approval was needed for your project. The UAB IRB cannot retrospectively approve projects; however, in this case, it appears that the UAB IRB approval would have been granted for this project had it been submitted for the UAB IRB review.

A copy of this memorandum will be sent to the graduate school and should serve as the final paperwork needed for your dissertation.

Cc: Julie Bryant, Graduate School

OMB No. 0990-0263
Approved for use through 07/31/2005

Protection of Human Subjects
Assurance Identification/IRB Certification/Declaration of Exemption
(Common Rule)

Policy: Research activities involving human subjects may not be conducted or supported by the Departments and Agencies adopting the Common Rule (56FR28003, June 18, 1991) unless the activities are exempt from or approved in accordance with the Common Rule. See section 101(b) of the Common Rule for exemptions. Institutions submitting applications or proposals for support must submit certification of appropriate Institutional Review Board (IRB) review and approval to the Department or Agency in accordance with the Common Rule. Institutions must have an assurance of compliance that applies to the research to be conducted and should submit certification of IRB review and approval with each application or proposal unless otherwise advised by the Department or Agency.

1. Request Type	2. Type of Mechanism	3. Name of Federal Department or Agency and, if known, Application or Proposal Identification No.
[X] ORIGINAL [ ] CONTINUATION [ ] EXEMPTION	[ ] GRANT [ ] CONTRACT [ ] FELLOWSHIP [ ] COOPERATIVE AGREEMENT [ ] OTHER:_____	
4. Title of Application or Activity Comprehensive Non-Invasive Assessment of Malignant Brain Tumor Angiogenesis: A Natural History Anatomic, Biochemical and Functional Imaging Study		5. Name of Principal Investigator, Program Director, Fellow, or Other NABORS, LOUIS BURT

6. Assurance Status of this Project *(Respond to one of the following)*

[X] This Assurance, on file with Department of Health and Human Services, covers this activity:
Assurance Identification No. FWA00005960, the expiration date 11/24/06 IRB Registration No. IRB00000196

[ ] This Assurance, on file with *(agency/dept)*_____, covers this activity.
Assurance No._____, the expiration date_____ IRB Registration/Identification No._____ *(if applicable)*

[ ] No assurance has been filed for this institution. This institution declares that it will provide an Assurance and Certification of IRB review and approval upon request.

[ ] Exemption Status: Human subjects are involved, but this activity qualifies for exemption under Section 101(b), paragraph_____.

7. Certification of IRB Review (Respond to one of the following IF you have an Assurance on file)

[X] This activity has been reviewed and approved by the IRB in accordance with the Common Rule and any other governing regulations.
by: [ ] Full IRB Review on (date of IRB meeting) or [X] Expedited Review on (date) 10-21-04
[ ] If less than one year approval, provide expiration date _____

[ ] This activity contains multiple projects, some of which have not been reviewed. The IRB has granted approval on condition that all projects covered by the Common Rule will be reviewed and approved before they are initiated and that appropriate further certification will be submitted.

8. Comments	Title
Please note: UAB IRB Protocol Number is X040924015 Protocol subject to Annual continuing review.	Comprehensive Non-Invasive Assessment of Malignant Brain Tumor Angiogenesis: A Natural History Anatomic, Biochemical and Functional Imaging Study

IRB Approval Issued: 11-09-04

9. The official signing below certifies that the information provided above is correct and that, as required, future reviews will be performed until study closure and certification will be provided.	10. Name and Address of Institution University of Alabama at Birmingham 701 20th Street South Birmingham, AL 35294
11. Phone No. *(with area code)* (205) 934-3789 12. Fax No. *(with area code)* (205) 934-1301 13. Email: smoore@uab.edu	
14. Name of Official Marilyn Doss, M.A.	15. Title Vice Chair, IRB
16. Signature Marilyn Doss	17. Date 10/21/04

Authorized for local Reproduction — Sponsored by HRS

Public reporting burden for this collection of information is estimated to average less than an hour per response. An agency may not conduct or sponsor, and a person is not required to respond to, a collection of information unless it displays a currently valid OMB control number. Send comments regarding this burden estimate or any other aspect of this collection of information, including suggestions for reducing this burden to: OS Reports Clearance Officer, Room 503 200 Independence Avenue, SW., Washington, DC 20201. *Do not return the completed form to this address.*

OMB No. 0990-0263
Approved for use through 07/31/2005

Protection of Human Subjects
Assurance Identification/IRB Certification/Declaration of Exemption
(Common Rule)

Policy: Research activities involving human subjects may not be conducted or supported by the Departments and Agencies adopting the Common Rule (56FR28003, June 18, 1991) unless the activities are exempt from or approved in accordance with the Common Rule. See section 101(b) of the Common Rule for exemptions. Institutions submitting applications or proposals for support must submit certification of appropriate Institutional Review Board (IRB) review and approval to the Department or Agency in accordance with the Common Rule. Institutions must have an assurance of compliance that applies to the research to be conducted and should submit certification of IRB review and approval with each application or proposal unless otherwise advised by the Department or Agency.

1. Request Type	2. Type of Mechanism	3. Name of Federal Department or Agency and, if known, Application or Proposal Identification No.
[ ] ORIGINAL [X] CONTINUATION [ ] EXEMPTION	[ ] GRANT [ ] CONTRACT [ ] FELLOWSHIP [ ] COOPERATIVE AGREEMENT [ ] OTHER:_____	

4. Title of Application or Activity	5. Name of Principal Investigator, Program Director, Fellow, or Other
NABTT 9911 - A Phase I/II Trial of EMD 121974 for Treatment of Patients With Recurrent Malignant Gliomas	NABORS, LOUIS BURT

6. Assurance Status of this Project *(Respond to one of the following)*

[X] This Assurance, on file with Department of Health and Human Services, covers this activity:
Assurance Identification No. FWA00005960, the expiration date 11/24/06 IRB Registration No. IRB00000196

[ ] This Assurance, on file with *(agency/dept)*_____, covers this activity.
Assurance No._____, the expiration date_____ IRB Registration/identification No._____ *(if applicable)*

[ ] No assurance has been filed for this institution. This institution declares that it will provide an Assurance and Certification of IRB review and approval upon request.

[ ] Exemption Status: Human subjects are involved, but this activity qualifies for exemption under Section 101(b), paragraph_____.

7. Certification of IRB Review (Respond to one of the following IF you have an Assurance on file)

[X] This activity has been reviewed and approved by the IRB in accordance with the Common Rule and any other governing regulations.
by: [X] Full IRB Review on (date of IRB meeting) 10/6/2004 or [ ] Expedited Review on (date)
[ ] If less than one year approval, provide expiration date _____

[ ] This activity contains multiple projects, some of which have not been reviewed. The IRB has granted approval on condition that all projects covered by the Common Rule will be reviewed and approved before they are initiated and that appropriate further certification will be submitted.

8. Comments	Title
Please note: UAB IRB Protocol Number is F000330001 Protocol subject to Annual continuing review. HIPAA Waiver Approved?: No IRB Approval Issued: 10-07-04	NABTT 9911 - A Phase I/II Trial of EMD 121974 for Treatment of Patients With Recurrent Malignant Gliomas

9. The official signing below certifies that the information provided above is correct and that, as required, future reviews will be performed until study closure and certification will be provided.	10. Name and Address of Institution
11. Phone No. *(with area code)* (205) 934-3789 12. Fax No. *(with area code)* (205) 934-1301 13. Email: smoore@uab.edu	University of Alabama at Birmingham 701 20th Street South Birmingham, AL 35294

14. Name of Official	15. Title
Ferdinand Urthaler, M.D.	Chairman, IRB

16. Signature	17. Date
Ferdinand Urthaler, MD	10-07-04

Authorized for local Reproduction — Sponsored by HHS

Public reporting burden for this collection of information is estimated to average less than an hour per response. An agency may not conduct or sponsor, and a person is not required to respond to, a collection of information unless it displays a currently valid OMB control number. Send comments regarding this burden estimate or any other aspect of this collection of information, including suggestions for reducing this burden to: OS Reports Clearance Officer, Room 503 200 Independence Avenue, SW., Washington, DC 20201. *Do not return the completed form to this address.*

OMB No. 0925-0418
Approved for use through 01/31/2001

Protection of Human Subjects
Assurance Identification/Certification/Declaration
(Common Federal Rule)

Policy: Research activities involving human subjects may not be conducted or supported by the Departments and Agencies adopting the Common Rule (56FR28003, June 18, 1991) unless the activities are exempt from or approved in accordance with the common rule. See section 101(b) the common rule for exemptions. Institutions submitting applications or proposals for support must submit certification or appropriate institutional Review Board (IRB) review and approval to the Department or Agency in accordance with the common rule.

Institutions with an assurance of compliance that covers the research to be conducted on file with the Department, Agency, or the Department of Health and Human Services (HHS) should submit certification of IRB review and approval with each application or proposal unless otherwise advised by the Department or Agency. Institutions which do not have such an assurance must submit an assurance and certification of IRB review and approval within 30 days of a written request from the Department or Agency.

1. Request Type	2. Type of Mechanism	3. Name of Federal Department or Agency and, if known, Application or Proposal Identification No.
☐ ORIGINAL ☐ FOLLOWUP ☐ EXEMPTION	☐ GRANT ☐ CONTRACT ☐ FELLOWSHIP ☐ COOPERATIVE AGREEMENT ☐ OTHER:	

4. Title of Application or Activity	5. Name of Principal Investigator,Program Director, Fellow, or Other
NABTT 9911 - A Phase I/II Trial of EMD 121974 for Treatment of Patients With Recurrent Malignant Gliomas	NABORS, LOUIS BURT

6. Assurance Status of this Project *(Respond to one of the following)*

☒ This Assurance, on file with Department of Health and Human Services, covers this activity:
Assurance identification no. M-1149 IRB identification no. 01

☐ This Assurance, on file with *(agency/dept)*_____, covers this activity.
Assurance identification no._____ IRB identification no._____ *(if applicable)*

☐ No assurance has been filed for this project. This institution declares that it will provide an Assurance and Certification of IRB review and approval upon request.

☐ Exemption Status: Human subjects are involved, but this activity qualifies for exemption under Section 101(b), paragraph_____

7. Certification of IRB Review (Respond to one of the following IF you have an Assurance on file)

☒ This activity has been reviewed and approved by the IRB in accordance with the common rule and any other governing regulations or subparts on *(date)* 12 13 02 by: ☒ Full IRB Review or ☐ Expedited Review

☐ This activity contains multiple projects, some of which have not been reviewed. The IRB has granted approval on condition that all projects covered by the common rule will be reviewed and approved before they are initiated and that appropriate further certification will be submitted.

8. Comments	Title
Please note: UAB IRB Protocol Number is F000330001 Protocol subject to Annual continuing review.	NABTT 9911 - A Phase I/II Trial of EMD 121974 for Treatment of Patients With Recurrent Malignant Gliomas

9. The official signing below certifies that the information provided above is correct and that, as required, future reviews will be performed and certification will be provided.	10. Name and Address of Institution
11. Phone No. *(with area code)*: (205) 934-3789 12. Fax No. *(with area code)*: (205) 934-1301	University of Alabama at Birmingham 701 20th Street South Birmingham, AL 35294
13. Name of Official: Ferdinand Urthaler, M.D.	14. Title: Chairman, IRB
15. Signature: Ferdinand Urthaler. M.D.	16. Date: 02-1902

Authorized for local Reproduction | OPTIONAL FORM 310 (Rev. 1-98) | Sponsored by HHS/NIH

Public reporting burden for this collection of information is estimated to average less than an hour per response. An agency may not conduct or sponsor, and a person is not required to respond to, a collection of information unless it displays a currently valid OMB control number. Send comments regarding this burden estimate or any other aspect of this collection of information, including suggestions for reducing this burden to: NIH, Project Clearance Office, 5701 Rockledge Drive, MSC 7730, Bethesda, Md. 20892-7730, ATTN: PRA 0925-0418. *Do not return the completed form to this address.*

OMB No. 0990-0263
Approved for use through 07/31/2005

Protection of Human Subjects
Assurance Identification/IRB Certification/Declaration of Exemption
(Common Rule)

Policy: Research activities involving human subjects may not be conducted or supported by the Departments and Agencies adopting the Common Rule (56FR28003, June 18, 1991) unless the activities are exempt from or approved in accordance with the Common Rule. See section 101(b) of the Common Rule for exemptions. Institutions submitting applications or proposals for support must submit certification of appropriate Institutional Review Board (IRB) review and approval to the Department or Agency in accordance with the Common Rule. Institutions must have an assurance of compliance that applies to the research to be conducted and should submit certification of IRB review and approval with each application or proposal unless otherwise advised by the Department or Agency.

1. Request Type	2. Type of Mechanism	3. Name of Federal Department or Agency and, if known, Application or Proposal Identification No.
[X] ORIGINAL [ ] CONTINUATION [ ] EXEMPTION	[ ] GRANT [ ] CONTRACT [ ] FELLOWSHIP [ ] COOPERATIVE AGREEMENT [ ] OTHER:_____	

4. Title of Application or Activity	5. Name of Principal Investigator, Program Director, Fellow, or Other
Comprehensive Non-invasive Assessment of Malignant Brain Tumor Angiogenesis: A Natural History Anatomic, Biochemical and Functional Imaging Study	NABORS, LOUIS BURT

6. Assurance Status of this Project *(Respond to one of the following)*

[X] This Assurance, on file with Department of Health and Human Services, covers this activity:
Assurance Identification No. FWA00005960, the expiration date 11/24/06 IRB Registration No. IRB00000196

[ ] This Assurance, on file with *(agency/dept)*_____, covers this activity.
Assurance No._____, *the expiration date*_____ *IRB Registration/Identification No.*_____ *(if applicable)*

[ ] No assurance has been filed for this institution. This institution declares that it will provide an Assurance and Certification of IRB review and approval upon request.

[ ] Exemption Status: Human subjects are involved, but this activity qualifies for exemption under: Section 101(b), paragraph_____.

7. Certification of IRB Review (Respond to one of the following IF you have an Assurance on file)

[X] This activity has been reviewed and approved by the IRB in accordance with the Common Rule and any other governing regulations.
by: [ ] Full IRB Review on (date of IRB meeting) or [X] Expedited Review on (date) 10-21-04
[ ] If less than one year approval, provide expiration date _____

[ ] *This activity contains multiple projects, some of which have not been reviewed. The IRB has granted approval on condition that all projects* covered by the Common Rule will be reviewed and approved before they are initiated and that appropriate further certification will be submitted.

8. Comments	Title
Please note: UAB IRB Protocol Number is X040924015 Protocol subject to Annual continuing review. IRB Approval Issued: 11-09-04	Comprehensive Non-invasive Assessment of Malignant Brain Tumor Angiogenesis: A Natural History Anatomic, Biochemical and Functional Imaging Study

9. The official signing below certifies that the information provided above is correct and that, as required, future reviews will be performed until study closure and certification will be provided.	10. Name and Address of Institution
11. Phone No. *(with area code)* (205) 934-3789 12. Fax No. *(with area code)* (205) 934-1301 13. Email: smoore@uab.edu	University of Alabama at Birmingham 701 20th Street South Birmingham, AL 35294

14. Name of Official	15. Title
Marilyn Doss, M.A.	Vice Chair, IRB

16. Signature: Marilyn Doss 17. Date 10/21/04

Authorized for local Reproduction — Sponsored by HHS

GRADUATE SCHOOL
UNIVERSITY OF ALABAMA AT BIRMINGHAM
DISSERTATION APPROVAL FORM
DOCTOR OF PHILOSOPHY

Name of Candidate Narasimha Shastry Akella

Graduate Program Biomedical Engineering

Title of Dissertation Assessment of Brain Tumor Angiogenesis Using Perfusion Magnetic Resonance Imaging and Magnetic Resonance Spectroscopy

I certify that I have read this document and examined the student regarding its content. In my opinion, this dissertation conforms to acceptable standards of scholarly presentation and is adequate in scope and quality, and the attainments of this student are such that he may be recommended for the degree of Doctor of Philosophy.

Dissertation Committee:

Name		Signature
Louis B. Nabors	**, Co-Chair**	
Donald B. Twieg	**, Co-Chair**	
Joel K. Cure		
Bradley R. Newcomer		
Edward G. Walsh		

Director of Graduate Program

Dean, UAB Graduate School

Date